Winter 2023

A Characterization of Hyporheic Temperatures with Applications for Salmon Habitat Restoration in a Thermally Impaired River

Sydney Jantsch
Western Washington University, sydneyjantsch@gmail.com

A Characterization of Hyporheic Temperatures with Applications for Salmon Habitat Restoration in a Thermally Impaired River

By

Sydney Jantsch

Accepted in Partial Completion
of the Requirements for the Degree
Master of Science

ADVISORY COMMITTEE

Dr. James M. Helfield, Chair

Dr. Kathryn L. Sobocinski

Dr. Leo Bodensteiner

GRADUATE SCHOOL

David L. Patrick, Dean

Master's Thesis

In presenting this thesis in partial fulfillment of the requirements for a master's degree at Western Washington University, I grant to Western Washington University the non-exclusive royalty-free right to archive, reproduce, distribute, and display the thesis in any and all forms, including electronic format, via any digital library mechanisms maintained by WWU.

I represent and warrant this is my original work, and does not infringe or violate any rights of others. I warrant that I have obtained written permissions from the owner of any third party copyrighted material included in these files.

I acknowledge that I retain ownership rights to the copyright of this work, including but not limited to the right to use all or part of this work in future works, such as articles or books.

Library users are granted permission for individual, research and non-commercial reproduction of this work for educational purposes only. Any further digital posting of this document requires specific permission from the author.

Any copying or publication of this thesis for commercial purposes, or for financial gain, is not allowed without my written permission.

Sydney Jantsch

11/17/23

A Characterization of Hyporheic Temperatures with Applications for Salmon Habitat Restoration in a Thermally Impaired River

A Thesis
Presented to
The Faculty of
Western Washington University

In Partial Fulfillment
Of the Requirements for the Degree
Master of Science

by
Sydney Jantsch
November 2023

Abstract

This thesis project is part of an ongoing study assessing the effectiveness of a potentially innovative habitat restoration strategy for Pacific salmon in thermally impaired rivers. This strategy uses engineered log jams (ELJs) to create pockets of cool-water refuge by forming deep scour pools and promoting localized upwellings of shallow subsurface (i.e., hyporheic) water. This project seeks to characterize the relationship between hyporheic temperature and overlying surface stream temperature to elucidate the extent to which hyporheic upwellings can deliver cool water to ELJ-formed pools during the summer low-flow season. Among six sites within a 2.7 km-long study reach on the South Fork Nooksack River, I found that one had hyporheic temperatures that were consistently colder than the overlying surface stream (categorized as "cold"), two had hyporheic temperatures that were variable but buffered relative to the overlying surface stream (categorized as "cool"), and three had hyporheic temperatures that were not buffered relative to the overlying surface stream (categorized as "warm"). The daily maximum and seven-day average of daily maximum temperatures at the cool sites were >1.5°C cooler in the hyporheic zone than the overlying surface stream, and at the cold site, the daily maximum was >8°C cooler. Yet the warm sites exhibited no meaningful differences between hyporheic and surface temperature. Similarly, the observed daily range in temperature was significantly smaller in the hyporheic zone at the cold and cool sites, but not at the warm sites. Habitat mapping around my study sites suggests it might be possible to identify well-buffered hyporheic flowpaths based on specific combinations of channel geomorphic units, which influence the length, extent, and depth of hyporheic flow paths. Building engineered log jams closer together and subsequently promoting closer spacing of

scour pools has the potential to greatly increase the extent of cool-water hyporheic upwellings in the South Fork. Conclusions drawn from this research can inform and improve the design of future habitat restoration efforts in a way that maximizes their benefit and promotes climate adaptation for salmon populations in thermally impaired rivers.

Acknowledgments

This research was conducted on the South Fork of the Nooksack River, part of the ancestral homelands of the Coast Salish Peoples, who have lived in the Salish Sea basin from time immemorial. I express my deepest respect and gratitude to our Indigenous neighbors, the Lummi Nation and Nooksack Tribe, for their enduring care and protection of our shared lands and waterways. I feel honored to share this land and help support the recovery of Chinook salmon.

I want to extend my gratitude to my thesis chair, Jim Helfield, for his knowledge, guidance, and belief in me. His support was unparalleled, and I couldn't have done it without him. I would also like to thank my field research assistant, Samantha Lopez, for her enthusiasm and hard work out on the river. She brought so much joy to this project. I want to thank my committee members, Leo Bodensteiner and Kathryn Sobocinski, for their time, assistance, and advice throughout this project. Andy Bunn and Audrey Salerno aided in the statistical analysis of my thesis adventure, and I am forever grateful; they really helped bring this research to the next level. I would also like to thank Mike Maudlin and Treva Coe of the Nooksack Indian Tribe Department of Natural Resources, and Kelley Turner, Nathan Rice, and Alex Levell at the Lummi Nation Department of Natural Resources for their continued partnership and support.

This research was funded by a U.S. Geological Survey Northwest Climate Adaptation Science Center award G17AC00218 to Sydney Jantsch. I would also like to acknowledge Western Washington University for providing funding, space, and equipment that helped make this research possible.

Table of Contents

List of Tables

List of Figures

Introduction

Pacific salmon *(Oncorhynchus* spp.) have been described as keystone species because of their importance as a food resource for predators and scavengers (Cederholm et al. 1989, Hilderbrand et al. 1999, Ford et al. 2010) and because of their role in transporting marine-derived nutrients to freshwater and terrestrial ecosystems (Willson et al. 1998, Lundberg and Moberg 2003, Helfield and Naiman 2006). Pacific salmon also play a crucial role as a cultural keystone species in Indigenous People's daily lives, contributing to their physical, social, economic, spiritual, psychological, and emotional well-being (Newell 1994, Carothers et al. 2021). The culture and identity of First Nations of the Pacific Northwest are inextricably tied to salmon and declines in the abundance of salmon greatly threaten the health of these communities. Over the past century, human actions have caused significant declines in salmon populations, and despite considerable efforts and expenditures for conservation and restoration, the prospects for salmon recovery remain unclear (Schoonmaker et al. 2003, Gustafson et al. 2007, Lackey 2022). Several stocks of Pacific salmon are listed as threatened or endangered under terms of the U.S. Endangered Species Act (NOAA 2015).

Elevated stream temperatures represent a major stressor affecting salmon populations and contribute to the impairment of numerous riverine ecosystems in the Pacific Northwest (Hashim and Bresler 2005, USEPA 2020). Elevated stream temperatures are caused by anthropogenic factors such as deforestation, water diversion, and urbanization, which entail reductions in shade and decreased infiltration of precipitation into groundwater (Poole and Berman 2001). This impairment will become increasingly severe and widespread in the coming

years due to global climate change, the effects of which include rising air temperatures as well as earlier and faster snowmelt and changes in streamflow generation, resulting in decreased summertime discharge (Mote et al. 2003, van Vliet et al. 2011). As lower flows entail decreased thermal capacity (Booker and Whitehead 2022), these hydrologic changes exert an important influence on stream temperatures, exacerbating the warming effects of rising air temperatures and loss of shade.

With regard to salmon, thermal impairment generally refers to the occurrence of warm water temperatures that are outside of the optimal habitat range. Temperature affects salmon at all life history stages: In incubating embryos, warmer stream temperatures increase the rate of development and alter the timing of emergence, with potentially adverse effects on survival rates (Bjornn and Reiser 1991). In fry, excessively warm temperatures ($\gtrapprox$25 °C) can result in acute mortality, while warm sublethal temperatures ($\gtrapprox$15 °C) affect standard and active metabolism so as to restrict the amount of energy that can be used for swimming and feeding, which hampers growth and makes fry more vulnerable to predators (McCullough et al. 2001). In returning adults, elevated temperatures induce stress responses and increase the virulence of pathogens, both of which can lead to premature mortality (von Biela et al. 2020). The latter effects are especially important in populations that undertake spawning migrations in summer, such as sockeye salmon (*O. nerka*; Hinch and Martins 2011) and early (i.e., spring- and summer-run) Chinook salmon (*O. tshawytscha*; Connor et al. 2019, Bowen et al. 2020).

A strategy that shows promise for allowing salmon populations to persist in thermally-impaired streams involves the construction of engineered log jams (ELJs). ELJs are human-made structures made of wood and other materials installed in streams to simulate naturally-

occurring large woody debris (LWD) jams, which fulfill several critical functions affecting fish habitat (Beechie and Sibley 1997, Gregory et al. 2003). In degraded streams, ELJs are frequently designed to deflect streamflow, which scours the adjacent streambed and enhances the development of deep, complex pools (Roni et al. 2008, Cramer 2012). Among other habitat benefits, deep wood-formed pools have greater thermal capacity and thus maintain cooler and more stable summertime temperatures relative to other habitat features (Elliott 2000), providing thermally-favorable holding water (i.e., cool-water refuge) for salmon. Access to such cool-water refuge can mitigate thermal stress sufficiently to improve growth and survival rates in juvenile salmon (Ebersole et al. 2001) and improve reproductive success in migrating adults (Benda et al. 2015). By allowing salmon to persist in thermally-impaired streams, ELJs may promote climate adaptation in threatened populations and serve as an essential component of a comprehensive strategy for salmon recovery.

ELJs may be most effective at providing cool-water refuge when ELJ-formed pools receive inputs from cool-water sources such as subsurface upwellings. At sites where such cool-water sources are not present, ELJ installation can alter the shape of the riverbed in a way that invites the potential for localized upwellings of cool water from the hyporheic zone. The hyporheic zone is the saturated area beneath and adjacent to the stream, where the water is a mixture of surface stream water and groundwater (Edwards 1998). Hyporheic flows tend to feature relatively cool and constant temperatures, and hyporheic inputs can thus moderate stream temperatures (Burkholder et al. 2008, Torgersen et al. 2012).

In coarse-bedded rivers during the summer low-flow season, a large proportion of total discharge may be carried through the hyporheic zone (Fernald et al. 2006), and significant

amounts of water may be exchanged between the hyporheic zone and the overlying surface stream. Hyporheic exchange is strongly influenced by streambed topography: Areas of upwelling, where water moves from the hyporheic zone to the surface stream, typically occur at the heads of pools, while areas of downwelling, where water moves from the surface stream into the hyporheic zone, typically occur at pool tailouts (Harvey and Bencala 1993, Edwards 1998). Spatial patterns and volumes of hyporheic exchange can thus be drastically altered by changes in bed topography (Tonina and Buffington 2007), which can be brought about by naturally-occurring LWD accumulations or ELJ construction. By promoting the development of scour pools in channels that were previously lacking pools, ELJs may promote localized upwellings. Previous studies have demonstrated the relationships between the presence of LWD, channel morphology, and hyporheic flow (Abbe and Montgomery 2003, Kasahara and Wondzell 2003, Mutz et al. 2007, Hester et al. 2009, Wondzell et al. 2009). Still, few data are available to assess the viability of using ELJs to promote localized upwellings and create cool-water refuge for salmon.

This research project is part of a collaboration between Western Washington University and the Nooksack Indian Tribe to assess the viability of using ELJs to promote localized upwellings and create cool-water refuge for early Chinook salmon in the lower South Fork Nooksack River (SF Nooksack). An underlying assumption of this restoration strategy is that hyporheic flows remain cooler and more stable than overlying surface water during the summer low-flow season. The specific objectives of my research are to test this assumption by characterizing the temporal and spatial relationships between hyporheic and overlying surface stream temperatures, and to elucidate the extent to which hyporheic upwellings can deliver

cool water to ELJ-formed pools during the summer low-flow season. The long-term goal of this work is to guide future habitat restoration efforts by determining the optimal placement of ELJs to maximize their ability to provide cool-water refuge and promote climate resiliency for early Chinook salmon and other fish populations threatened by elevated stream temperatures.

Methods

Study Sites

The SF Nooksack is a tributary of the Nooksack River in northwestern Washington state, USA (Figure 1). It's Nooksack place name is *Nuxw7íyem*, which translates as "always clear water" (NNR 2012). It drains approximately 425 km^2 (164 mi^2) of watershed area before it meets with the North Fork Nooksack River, the northernmost river in Washington, to form the main stem of the Nooksack River (Grah et al. 2017). The headwaters of the SF Nooksack arise in snowfields on Twin Sisters Mountain, *Kwetl'kwítl' Smánit*, the melting of which sustains river flows throughout the beginning of the summer. This winter mountain snowpack generally melts in June and July, after which river flow is sustained primarily by groundwater inflow (Gendaszek 2014, Grah et al. 2017). River flows decrease throughout August and early September, during the time of year when air temperatures are typically warmest (Figure 2). As a consequence of climate change, the North Cascades are experiencing lower snowfall, and the snowpack on the Twin Sisters is melting faster each year, decreasing the amount of water flowing into the SF Nooksack during the summer low flow season (Grah et al. 2017). The combination of decreased snowpack, earlier melt-off, and rising summer air temperatures leads to a prolonged low-flow

season with increasing water temperatures and diminished water flow, a condition that is likely to be exacerbated in years to come (Yoder and Raymond 2022).

The SF Nooksack basin is situated in a second-growth mixed conifer-hardwood forest dominated by Douglas fir (*Pseudotsuga menziesii)* and western redcedar (*Thuja plicata)*, which account for nearly 70% of the woody species in the basin (Grah et al. 2017). Black cottonwood (*Populus trichocarpa*), willows (*Salix* spp.*)*, and red alder (*Alnus rubra*) are common deciduous trees that grow in the floodplain (Grah et al. 2017). Predominant land uses in the watershed include logging in the headwaters, as well as livestock farming and other agricultural operations such as berry fields, Christmas tree plantations, hayfields, and corn in the lower reaches (Grah et al. 2017). Streamside forest clearing associated with agricultural practices in the lower watershed has resulted in decreased canopy coverage and correspondingly increased water temperatures. The lack of riparian buffer also contributes to a scarcity of LWD and LWD-formed pools, with a corresponding scarcity of cool-water refuge habitat (Maudlin et al. 2002, Soicher et al. 2006). The streambed is composed mainly of coarse gravel and cobble alluvium, with some boulders and exposed bedrock. Coarse-scale measurements indicate hydraulically conductive substrates with ample potential for hyporheic exchange (Gendaszek 2014).

The SF Nooksack supports all seven North American species of Pacific salmon: Chinook salmon, chum salmon (*O. keta*), coho salmon (*O. kisutch*), pink salmon (*O. gorbuscha*), sockeye salmon, cutthroat trout (*O. clarkii*), and steelhead (*O. mykiss*; USEPA 2016a). The SF Nooksack includes a vast network of salmon streams, with salmon observed 51 river km (32 river miles) upstream of its confluence with the North Fork (Pelto et al. 2022). The lower SF Nooksack is a priority area for salmon habitat restoration (WRIA 1 SRB 2005) because it supports an

endangered population of early Chinook salmon that is considered essential for the recovery of the broader Puget Sound Chinook salmon evolutionarily significant unit (ESU), which is listed as threatened under the U.S. Endangered Species Act (ESA; Maudlin et al. 2002, Soicher et al. 2006, Butcher et al. 2016, USEPA 2016b). The SF Nooksack early Chinook salmon enter the river as adults in Spring and spawn in mid-August through September, holding for long periods when river temperatures are at their warmest (Maudlin et al. 2002). As a consequence, the population is imperiled by elevated stream temperatures that are exacerbated by low flows during the summer (Grah et al. 2017).

Nesset's Reach Habitat Restoration

This research project was conducted within the Nesset's Reach section of the lower SF Nooksack (48.692019 ° N, -122.164114 ° W; Figure 1). Nesset's Reach is approximately 2.7 km long, located near Acme, Washington, approximately 17 river km (10 river miles) above the confluence with the North Fork. In 2016 and 2018, the Nooksack Indian Tribe Natural Resources Department (NNR) installed a series of ELJs in Nesset's Reach (NNR 2015, NNR 2016). Phase 1 of the project involved the construction of a total of 20 ELJs in a 0.8 km stretch of river, five of which are included in my study. Phase 2 involved the construction of an additional five ELJs in a 0.5 km river segment further downstream, of which one is included in my study. The principal objective of the NNR Nesset's Reach ELJ project was to provide cool-water refuge for adult early Chinook salmon by creating deep and complex scour pools. Preliminary evidence suggests that these ELJs have been effective at creating deep pools and enhancing localized upwellings of

hyporheic flow, and that the resulting ELJ-formed pools are used for holding by adult early Chinook salmon (J. Helfield and NNR, *unpublished data*).

Experimental Design and Data Collection

To characterize the relationship between hyporheic and surface stream temperatures, I measured water temperature simultaneously in the hyporheic zone and the overlying surface stream at six study sites within Nesset's Reach. Each site consisted of a single ELJ and an associated ELJ-formed pool with a riffle immediately upstream. Each study site was assigned an identification number that corresponded to the identification number of the NRR ELJ structure: 1302, 1306, 1312, 1313, 1316, and 2124 (Table 1; Figure 1). All temperatures were measured using temperature loggers with ± 0.2 °C precision (TidBit v2 Temp logger, Onset Computer Corporation, Bourne, MA). At each site, hyporheic temperatures were measured with a single logger deployed inside a piezometer in an upwelling zone at the riffle tail/pool head, at a depth of approximately 35 cm below the streambed. The corresponding surface stream temperatures were measured with a second logger deployed on the streambed <1 m upstream of the piezometer. At each site, the two loggers were programmed to record water temperature simultaneously every hour during the summer low flow season (August 6 - September 13, 2022).

To accommodate temperature loggers that were approximately 2.54 cm (1") in diameter, I fabricated a custom piezometer installation apparatus, following the general design described by Baxter et al. (2003). Each piezometer consisted of a 1.2-1.5 m length of schedule 40 polyvinyl chloride (PVC) pipe with an outside diameter of 4.2 cm and an inside diameter of

3.5 cm (nominal size 1 ¼"). Each piezometer was plugged at the bottom and had 14 holes in the sidewall that were 0.3175 cm (1/8") in diameter. The holes were equally spaced over the bottom 10 cm of the piezometer's length, allowing hyporheic water to flow through the piezometer. The holes were covered with a fine (200-μm) mesh sleeve to reduce sediment inputs inside the piezometer. To facilitate measurements of installation depth, the piezometers were graduated and labeled.

At each site, I measured temperatures at the riffle tail/pool head because this location has the greatest potential of being in an upwelling zone. This was to ensure that temperature measurements were collected in upwelling or neutral areas, which contain the largest proportion of hyporheic flow, as opposed to downwelling areas, which contain a greater proportion of recent surface stream water. To install each piezometer into the substrate, I used a 1.2 m-long driving rod made of 4.4 cm-diameter (nominal size 1 ¾") cold-rolled steel fitted with a 6 cm-diameter steel cap, and a 1.14 m-long driving sleeve made of stainless-steel pipe with an inside diameter of 4.6 cm and an outside diameter of 5 cm (nominal size 2"). Following procedures described by Baxter et al. (2003), the driving rod was inserted into the sleeve, and the rod and sleeve were pounded into the substrate together using a 1.8-kg (4-lb.) sledgehammer. Once driven down to the appropriate depth, the rod was removed from inside the sleeve, and a piezometer was inserted in its place. The sleeve was then removed from around the piezometer, leaving the piezometer inserted into the substrate. Precise installation depths were measured and recorded for each piezometer (Table 1).

Throughout this project, I developed and refined my procedures and apparatus for installing piezometers in a coarse-bedded river. In some sites, I found it necessary to use open-

bottom piezometers with no sidewall perforations, into which I inserted a 2.5 cm diameter steel driving rod with a 6-cm diameter steel cap and pounded on the cap to drive the rod and piezometer into the substrate simultaneously. This process was faster, required fewer field materials, and was less likely to result in sand and silt being lodged between the driving rod and sleeve, which made piezometer installation difficult at some sites. The open-bottom piezometers measured hydraulic head at the bottom opening of the piezometer, approximately 35 cm below the streambed, over an area equal to that of a circle with a diameter equal to the piezometer's inside diameter (i.e., 9.62 cm^2). In contrast, the perforated, closed-bottom piezometers integrated hydraulic head measurements within a column of water extending 10 cm above the bottom of the piezometer, approximately 25 to 35 cm below the streambed. This column was equal in volume to the length of the sidewall perforations multiplied by the inside area of the piezometer (i.e., 10 cm x 9.62 cm^2 = 96.2 cm^3). This difference in piezometer apparatus may have had a subtle effect on hydraulic head measurements, but it likely did not affect hyporheic temperature measurements, as temperatures were measured at comparable depths at the bottoms of both closed- and open-bottomed piezometers. The closed-bottom piezometers were deployed at two of the six study sites (1302 and 2124), and the open-bottom piezometers were used at the other four sites (1306, 1312, 1313, and 1316).

Following installation, I used a hand-held vacuum pump (Mityvac model MV8000, SKF Lubrication Systems USA Inc., St. Louis, MO) to remove water and fine sediment inside the piezometer. For each piezometer, pumping continued until at least 2 L of water had been removed and the pumped water was visibly clear. This was to remove any surface water that

may have entered the piezometer during installation and to ensure a connection with the hyporheic zone.

After the piezometer was left to equilibrate for 24 hours, I measured the upwelling potential at the installation location. Upwelling potential was characterized in terms of vertical hydraulic gradient (VHG), which is a unitless measure of the pressure differential between the hyporheic zone at a given location and the overlying surface stream (Dahm and Valett 1996). VHG is calculated as follows:

$$VHG = (h_s - h_p) / L$$

where h_s is the height of the top of the piezometer above the water level of the surface stream (cm), h_p is the height of the top of the piezometer above the water level within the piezometer (cm), and L is the depth from the streambed to the first opening in the piezometer (cm). Positive VHG values indicate upwelling potential, negative VHG values indicate downwelling potential, and a zero VHG value indicates no hyporheic exchange (Dahm and Valette 1996). I used an electronic water level meter (Model 102M Mini Water Level Meter, Solinst Canada Ltd., Georgetown, ON) to measure water levels. To account for fluctuations in surface water level due to turbulent streamflow, I measured h_s inside a 3.5 cm-diameter stilling well (i.e., a length of open-bottomed PVC pipe) attached to the outside of the piezometer, extending vertically from the top of the piezometer to a depth below the stream surface but above the streambed. Table 1 lists VHG values observed at each site and piezometer installation depths.

Once I confirmed that upwellings were present at each site, I installed a temperature logger at the bottom of the piezometer. I then installed another temperature logger on the streambed <1 m upstream from the piezometer. Each streambed temperature logger was

housed inside a short (5-8 cm) length of 4 cm-diameter (nominal 1 ¼") schedule 40 PVC, which was perforated all over to allow water flow. This housing was then placed inside a 30-35 cm length of 8.9 cm-diameter (nominal 3") schedule 40 PVC conduit that was also perforated all over and filled with river rocks that acted as an anchor to keep the logger in place throughout the season. Once assembled and placed on the streambed, each PVC housing was covered with river rocks for camouflage. Periodically, I visited the sites to confirm that the piezometers and streambed housings were still in position. During that time, I used a data shuttle (HOBO Waterproof Shuttle, Onset Computer Corporation, Bourne, MA) to download the data collected thus far.

To help identify geomorphic factors that might influence patterns of hyporheic temperature, I measured thalweg depths and surveyed channel geomorphic units (CGUs) throughout Nesset's Reach. These habitat surveys were conducted during the low flow season (August 2022), following NNR protocols for monitoring habitat restoration projects (Coe 2019).

Data Analysis

To characterize trends over time in hyporheic and surface stream temperature, I performed permutation tests to analyze the difference in mean temperature between the surface stream and the underlying hyporheic zone for each hour of the day at each site. Hourly temperatures were averaged across all days in the sample period. For each hour at each site, I compared the observed differences against a distribution of permuted differences, based on 1,000 permutations. In cases where a difference equal to or greater than the observed

difference occurred in fewer than 5% of permutations, the difference was deemed statistically significant.

At each site, I characterized hyporheic and surface temperatures according to three response variables: daily maximum, seven-day average of the daily maximum (7DADM), and daily range. I calculated the daily maximum as the maximum temperature recorded during a 24-hour period (12:00 am – 11:59 pm). I calculated 7DADM as a moving average in which the daily maximum value for a given day was averaged with the daily maximum values of the previous three days and the following three days. I calculated the daily range as the difference between the daily maximum and minimum temperature recorded during a given 24-hour period. To assess differences in these response variables between the hyporheic zone and the overlying surface stream, I performed paired t-tests and calculated the difference in means at each study site. Shapiro-Wilks tests indicated that the data met assumptions of normality ($p<0.05$). To assess the relationships between each response variable and potential confounding variables, I conducted regression analyses using linear models across all sites with each response variable as a function of either VHG or installation depth. All analyses were conducted in R version 4.2.2 (R Core Team 2022).

Results and Discussion

The relationship between hyporheic temperature and overlying surface stream temperature is variable over small spatial scales. Not all sites featured hyporheic flows that were cooler or more stable than the overlying surface stream water during the summer low-flow season (Figures 3-8). Permutation tests indicate that the diel relationship between

hyporheic and overlying surface stream temperature varies among sites (Table 2). At site 1316, the hyporheic zone was significantly cooler at every hour of the day, whereas at sites 1302 and 1306 the hyporheic zone was significantly cooler during part of the day: At site 1302, the hyporheic zone was cooler for the majority of the day (i.e., between the hours of 10:00 am and 2:00 am), and at site 1306, the hyporheic zone was cooler throughout the morning (5:00 – 11:00 am), and in the afternoon and evening (2:00 – 9:00 pm). Conversely, there were no significant differences in temperature between the hyporheic zone and the surface stream at any hour of the day at sites 1312, 1313, and 2124. At site 1302, the hyporheic and surface stream temperatures converged towards the end of the season (Figure 3), when discharge was at its lowest (Figure 2). This is likely due to the fact that, as the summer progresses and the water level decreases, hyporheic upwellings account for a larger proportion of total streamflow. As a result, the surface temperature pattern is controlled to a greater extent by the hyporheic temperature pattern.

Based on these observed temperature patterns, I grouped the six study sites into three hyporheic temperature categories: cold, cool, and warm. The cold category represents the site where hyporheic temperatures are consistently colder than the overlying surface stream temperature during the low-flow season (1316). At site 1316, hyporheic temperatures averaged 11.7 °C and never exceeded 13.0 °C, while surface stream temperatures averaged 18 °C (Figure 7). The cool category denotes sites where hyporheic temperatures are variable but generally buffered relative to overlying surface stream temperatures (1302 and 1306), and the warm category denotes the sites where hyporheic temperatures are not buffered relative to overlying surface temperatures (1312, 1313, and 2124).

The cold, cool, and warm categories also serve to characterize hyporheic temperature in terms of daily maxima. Results from paired t-tests comparing hyporheic and surface stream temperatures indicate no significant difference in daily maximum temperature at the warm-classified site 2124, while at the other two warm-classified sites (1312 and 1313) the daily maximum was actually slightly warmer in the hyporheic zone (Table 3; Figure 9). These sites feature upwellings that are unlikely to create cool-water refuge and may even contribute to warming surface stream temperatures. Conversely, the hyporheic daily maximum was significantly cooler at each of the cold- and cool-classified sites. During the summer low-flow period, when surface stream temperatures warmed to approximately 20 °C on average, the maximum hyporheic temperature was approximately 18 °C at sites 1302 and 1306 (i.e., >1.6 °C cooler), and <11.7 °C at site 1316 (i.e., >8 °C cooler; Table 3).

I observed a similar trend in 7DADM (Figure 10). The difference between hyporheic and overlying surface stream 7DADM was statistically significant at all sites, but hyporheic 7DADM was slightly warmer at each of the warm-classified sites (1312, 1313, and 2124; Table 4). In contrast, the mean hyporheic 7DADM was >1.6 °C cooler at the cool-classified sites (1302 and 1306) and 8.6 °C cooler at the cold-classified site (1316; Table 4).

These differences have potentially important implications for the provision of cool-water refuge. In Pacific Northwest rivers, cool-water refuge is generally defined as an area >2 °C cooler than the mainstem flow (Torgersen et al. 2012). This difference might not be meaningful in cases where the mainstem flow is significantly warmer than the thermal optima of salmon, but the patterns observed in this study suggest that the difference between hyporheic and surface temperatures may in some cases align with the differences between stressful and non-

stressful conditions. For early Chinook salmon, thermal blockages to adult migration occur in the temperature range of 19-24 °C (Richter and Kolmes 2005, McCullough et al. 2011). When surface stream temperatures are within this range, hyporheic upwellings at cold- and cool-classified sites deliver water temperatures that are below it.

As with daily maxima, diel variation in temperature was lower at cold- and cool-classified sites, but not at warm-classified sites (Figure 11). Paired t-test results for the daily temperature range indicate that two of the warm-classified sites (1313 and 2124) had no significant differences between hyporheic and overlying surface water, while at the other warm site (1312), the daily temperature range was slightly greater in the hyporheic zone (Table 5). In contrast, results from the cool- and cold-classified sites indicate significantly less variable hyporheic temperatures with a difference in means of >1.5°C at the cool sites (1302 and 1306) and >3.5°C at the cold site (1316; Table 5).

The patterns I observed were likely not confounded by variations in sampling depth or upwelling potential. Although piezometer installation depths ranged from 30.5 to 37.5 cm and the magnitude of upwelling potential (VHG) ranged from 0.25 to 2.5 among sites (Table 1), regression analyses indicate no significant influence of installation depth or VHG on any response variable (Table 6).

The differences in the hyporheic-surface stream temperature relationship observed among my study sites are likely driven by differences in the length, extent, and depth of the hyporheic flow paths. Longer and deeper flow paths tend to be more stable and generally cooler during the summer low-flow season when river temperatures are at their greatest, but

increased flow path lengths also correspond to lower concentrations of dissolved oxygen (Edwards 1998, Fernald et al. 2006). Differences in water quality along hyporheic flow paths, including changes in temperature and dissolved oxygen concentration, also vary with differing degrees of hyporheic flow rates. For example, in the Willamette River in Oregon, Fernald et al. (2006) reported that greater hyporheic flow rates carry dissolved oxygen further distances and are more likely to propagate cooling at hyporheic upwellings.

Variations in hyporheic flow paths among study sites may be driven by variations in channel geomorphology. Channel geomorphology impacts water depth and velocity and may exert a significant impact on the location and magnitude of hyporheic exchange, as well as the depths and flow rates of hyporheic flow paths, which in turn affect hyporheic temperatures (Fernald et al. 2006). In Nesset's Reach, the cold and cool sites all occur where the riffle at the head of the ELJ-formed pool is immediately below another pool, whereas the warm sites all occur where the riffle is immediately below a run (Figure 12). This pattern aligns with findings observed in previous studies (Fernald et al. 2006, Gariglio et al. 2013): When a pool transitions to a riffle, the spatial gradient in depth and velocity is steep, which forces more water down into the hyporheic zone, resulting in greater hyporheic flow and deeper flow paths downstream. In contrast, when a run transitions into a riffle, the spatial gradient in depth and velocity is less steep, resulting in diminished and shallow hyporheic flow paths (Figure 13). Although sampling depth and VHG do not affect the patterns of hyporheic temperature observed at my study sites, the cooler and more stable flow paths may originate at greater depths or carry more hyporheic flow further upstream. Consequently, the temperature of

hyporheic flowpaths may be determined by specific combinations of channel geomorphic units upstream.

Conclusions and Recommendations

My findings indicate that hyporheic water temperatures are not always cooler or less variable compared to the overlying surface stream during the low flow season, and hyporheic temperatures can vary over relatively small spatial scales (i.e., within 0.5 km). My findings also suggest that this variability may be largely driven by easily observed patterns of channel morphology. These findings may be helpful in informing habitat restoration strategies in thermally-impaired rivers.

Given the significant spatial variation in hyporheic temperatures within a reach, an understanding of the location of cooler flowpaths is essential for restoration strategies that use hyporheic upwellings to provide cool-water refuge. Restoration managers may spend considerable time, funds, and effort installing ELJs in areas where hyporheic flowpaths are not buffered relative to the overlying surface stream. This could provide benefits for salmon through the creation of deep scour pools, which provide energetically-favorable holding water and have higher thermal capacity, but the comparatively warm hyporheic inputs will not contribute to the development of cool-water refuge.

The depth, flow rate, and length of hyporheic flow paths are vital pieces of information to collect at potential project sites to help inform where to install engineered log jams for maximum benefit. Obtaining these data can be highly time-consuming and consequently expensive, but my research offers the possibility of a shortcut. Restoration managers might be

able to improve the efficacy of ELJ restoration projects by utilizing easily obtained habitat mapping data. My results suggest that hyporheic flow paths are more likely to be well buffered downstream of a reach where a pool flows into a riffle. When a run is situated immediately upstream from a riffle, the underlying hyporheic flowpaths and potential upwellings downstream are likely to be less buffered. Consequently, building ELJs closer together and thereby promoting closer spacing of scour pools has the potential to greatly increase the extent of cool-water hyporheic upwellings at ELJ-formed pools.

There is likely an optimal flow path length that can provide maximum cool water inputs with adequate dissolved oxygen concentrations to support the temperature and dissolved oxygen requirements of salmon. Further research to identify the optimal flow path length would help inform where to install ELJs to maximize the benefits of upwellings and the subsequent extent of cool-water refuge. Mixing lengths within ELJ-formed pools might also exert an important influence on the extent to which upwellings can enhance cool-water refuge. Temperatures are likely to remain cooler at the bottoms of ELJ-formed pools in areas where mixing is inhibited by structural features such as logs or gravel accumulations that deflect the main flow away from the pool (Keller and Hofstra 1983), or where pools stratify vertically (Tate et al. 2007). The high variability observed among sites in this study illustrates the importance of researching and understanding the dynamics of hyporheic exchange in a way that can be applied to advance restoration efficacy.

Findings from this research can help river restoration managers revise current restoration protocols and improve the efficacy of future habitat restoration efforts. Installing ELJs in a way that enhances the potential for cool, hyporheic upwellings can greatly benefit

threatened salmon populations in thermally-impaired rivers, contributing to increased survival rates at all life history stages. Enhancing salmon habitat restoration and carefully selecting the ideal location for ELJ construction can increase the climate resiliency of early Chinook and other salmon populations, positively impacting the ecosystems they inhabit and the communities that value and depend on them.

Literature Cited

Abbe, T. B., and D. R. Montgomery. 2003. Patterns and processes of wood debris accumulation in the Queets River basin, Washington. *Geomorphology* 51: 81–107.

Baxter, C.V., F.R. Hauer, and W.W. Woessner. 2003. Measuring groundwater–stream water exchange: new techniques for installing minipiezometers and estimating hydraulic conductivity. *Transactions of the American Fisheries Society* 132: 493–502.

Beechie, T.J., and T.H. Sibley. 1997. Relationships between channel characteristics, woody debris, and fish habitat in northwestern Washington streams. *Transactions of the American Fisheries Society* 126: 217-229.

Benda, S.E., G.P. Naughton, C.C. Caudill, M.L. Kent, and C.B. Schreck. 2015. Cool, pathogen-free refuge lowers pathogen-associated prespawn mortality of Willamette River Chinook salmon. *Transactions of the American Fisheries Society* 144: 1159-1172.

Bjornn, T.C., and D.W. Reiser. 1991. Habitat requirements of salmonids in streams. *American Fisheries Society Special Publication* 19: 83-138.

Booker, D. J., and Whitehead, A. L. 2022. River water temperatures are higher during lower flows after accounting for meteorological variability. *River Research and Applications* 38: 3– 22.

Bowen, L., von Biela, V. R., McCormick, S. D., Regish, A. M., Waters, S. C., Durbin-Johnson, B., Britton, M., Settles, M. L., Donnelly, D. S., Laske, S. M., Carey, M. P., Brown, R. J., & Zimmerman, C. E. 2020. Transcriptomic response to elevated water temperatures in

adult migrating Yukon River Chinook salmon (*Oncorhynchus tshawytscha*). *Conservation Physiology* 8(1): coaa084.

Burkholder, B.K., G.E. Grant, R. Haggerty, T. Khangaonkar, and P.J. Wampler. 2008. Influence of hyporheic flow and geomorphology on temperature of a large, gravel-bed river, Clackamas River, Oregon, USA. *Hydrological Processes* 22: 941-953.

Butcher, J.B., M. Faizullabhoy, H. Nicholas, P. Cada, and J.T. Kennedy. 2016. Quantitative Assessment of Temperature Sensitivity of the South Fork Nooksack River under Future Climates using QUAL2Kw. U.S. Environmental Protection Agency, EPA/600/R-14/233, Washington, DC.

Carothers, C., J. Black, S. J. Langdon, R. Donkersloot, D. Ringer, J. Coleman, E. R. Gavenus, W. Justin, M. Williams, F. Christiansen, J. Samuelson, C. Stevens, B. Woods, S. J. Clark, P. M. Clay, L. Mack, J. Raymond-Yakoubian, A. A. Sanders, B. L. Stevens, and A. Whiting. 2021. Indigenous peoples and salmon stewardship: a critical relationship. *Ecology and Society* 26: 16.

Cederholm C.J., Houston D.B., Cole D.L., and W.J. Scarlett. 1989. Fate of coho salmon (*Oncorhynchus kisutch*) carcasses in spawning streams. *Canadian Journal of Fisheries and Aquatic Sciences* 46: 1347–135.

Coe, T. 2019. Quality Assurance Project Plan for Implementation and Effectiveness Monitoring of Nooksack River Watershed Habitat Restoration Projects. Revision 1: June 30, 2019. Nooksack Indian Tribe Natural Resources Department, Deming, WA.

Connor, W. P., K. F. Tiffan, J. A. Chandler, D. W. Rondorf, B. D. Arnsberg, and K. C. Anderson. 2019. Upstream migration and spawning success of Chinook salmon in a highly developed, seasonally warm river system. *Reviews in Fisheries Science & Aquaculture* 27: 1–50.

Cramer, M.L. (ed.). 2012. Stream Habitat Restoration Guidelines. Washington Departments of Fish and Wildlife, Natural Resources, Transportation and Ecology, Washington State Recreation and Conservation Office, Puget Sound Partnership, and U.S. Fish and Wildlife Service, Olympia, WA.

Dahm, C.N., and H.M. Valett. 1996. Hyporheic zones. Pages 107-119 *in* F.R. Hauer and G.A. Lamberti (eds.), Methods in Stream Ecology. Academic Press, San Diego, CA.

Ebersole, J.L., W.J. Liss, and C.A. Frissell. 2003. Cold water patches in warm streams: physicochemical characteristics and the influence of shading. *Journal of the American Water Resources Association* 39: 355-368.

Edwards, R.T. 1998. The hyporheic zone. Pages 399 – 429 *in* R.J. Naiman and R.E. Bilby (eds.), River Ecology and Management: Lessons from the Pacific Coastal Ecoregion. Springer-Verlag, New York.

Elliott, J.M. 2000. Pools as refugia for brown trout during two summer droughts: trout responses to thermal and oxygen stress. *Journal of Fish Biology* 56: 938-948.

Fernald, A. G., Landers, D. H., & Wigington Jr, P. J. 2006. Water quality changes in hyporheic flow paths between a large gravel bed river and off-channel alcoves in Oregon, USA. *River Research and Applications* 22: 1111–1124.

Ford, J.K., G.M. Ellis, P.F. Olesiuk, and K.C. Balcomb. 2010. Linking killer whale survival and prey abundance: food limitation in the oceans' apex predator? *Biology Letters* 6: 139-142.

Gariglio, F. P., Tonina, D., and C. H. Luce. 2013. Spatiotemporal variability of hyporheic exchange through a pool-riffle-pool sequence. *Water Resources Research* 49: 7185–7204.

Gendaszek, A., 2014. Hydrogeologic Framework and Groundwater/Surface-water Interactions of the South Fork Nooksack River Basin, Northwestern Washington. U.S. Geological Survey Scientific Investigations Report 2014–5221.

Grah, O., O'Neil, H., and Coe, T. 2017. South Fork Nooksack River Watershed Conservation Plan. Nooksack Indian Tribe Natural Resources Department, South Fork Nooksack Watershed Conservation Plan.

Gregory, S.V., K.L. Boyer, and A.M. Gurnell (eds.). 2003. The Ecology and Management of Wood in World Rivers. American Fisheries Society, Symposium 37, Bethesda, MD.

Gustafson, R.G., R.S. Waples, J.M. Myers, L.A. Weitkamp, G.J. Bryant, O.W. Johnson, and J.J. Hard. 2007. Pacific salmon extinctions: quantifying lost and remaining diversity. *Conservation Biology* 21: 1009-1020.

Harvey, J.W., and K.E. Bencala. 1993. The effect of streambed topography on surface-subsurface water exchange in mountain catchments. *Water Resources Research* 29: 89-98.

Hashim, W.A., and H. Bresler. 2005. Washington's Water Quality Management Plan to Control Nonpoint Source Pollution. Washington Department of Ecology Publication No. 05-10-027, Olympia, WA.

Helfield J.M., and R.J. Naiman. 2006. Keystone interactions: salmon and bear in riparian forests of Alaska. *Ecosystems* 9: 167-180.

Hester, E.T., M.W. Doyle, and G.C. Poole. 2009. The influence of in-stream structures on summer water temperatures via induced hyporheic exchange. *Limnology and Oceanography* 54: 355-367.

Hilderbrand G.V., Schwartz C.C., Robbins C.T., Jacoby M.E., Hanley T.A., Arthur S.M., and C Servheen. 1999. The importance of meat, particularly salmon, to body size, population productivity, and conservation of North American brown bears. *Canadian Journal of Zoology* 77: 132–8.

Hinch, S.G. and E.G. Martins. 2011. A review of potential climate change effects on survival of Fraser River sockeye salmon and an analysis of interannual trends in en route loss and pre-spawn mortality. Cohen Commission Tech. Rept. 9, Vancouver, B.C.

Kasahara, T., and S.M. Wondzell. 2003. Geomorphic controls on hyporheic exchange flow in mountain streams. *Water Resources Research* 39: 1005.

Keller, E.A., and T.D. Hofstra. 1983. Summer cold pools in Redwood Creek near Orick, California, and their importance as habitat for anadromous salmonids. Pages 221-224 *in* Proceedings of First Biennial Conference of Research in California National Parks. U.S. National Park Service, Cooperative Park Studies Unit, Davis, CA.

Lackey, R.T. 2022. The great Pacific Northwest salmon conundrum. Water Resources IMPACT. 24: 5-8. Lundberg J., and F. Moberg. 2003. Mobile link organisms and ecosystem functioning: implications for ecosystem resilience and management. *Ecosystems* 6: 87–98.

Maudlin, M., T. Coe, N. Currence, and J. Hansen. 2002. South Fork Nooksack River Acme-Saxon Reach Restoration Planning: Analysis of Existing Information and Preliminary Recommendations. Lummi Nation Natural Resources Department. Bellingham, WA.

McCullough, D., S. Spalding, D. Sturdevant, and M. Hicks. 2001. Issue Paper 5. Summary of Technical Literature Examining the Physiological Effects of Temperature on Salmonids. EPA-910-D-01-005, U.S. Environmental Protection Agency Region 10, Seattle, WA.

Mote, P.W., E.A. Parson, A.F. Hamlet, W.S. Keeton, D. Lettenmaier, N. Mantua, E.L. Miles, D.W. Perterson, D.L. Peterson, R. Slaughter, and A.K. Snover. 2003. Preparing for climate change: the water, salmon, and forests of the Pacific Northwest. *Climate Change* 61: 45–88.

Mutz, M., E. Kalbus, and S. Meinecke. 2007. Effect of instream wood on vertical water flux in low-energy sand bed flume experiments. *Water Resources Research* 43: W10424.

National Oceanic and Atmospheric Administration (NOAA). 2015. Status review update for Pacific salmon and steelhead listed under the Endangered Species Act: Pacific Northwest. Northwest Fisheries Science Center. Seattle, WA.

Newell, D. 1994. Tangled Webs of History: Indians and the Law in Canada's Pacific Coast Fisheries. University of Toronto Press, Toronto, Ont.

Nooksack Indian Tribe Natural Resources Department (NNR). 2012. South Fork Nooksack (Nuxw7íyem) Nesset Reach Design. Salmon Recovery Funding Board Project #12-1511. Washington State Recreation and Conservation Office, Olympia, WA, available at https://srp.rco.wa.gov/project/360/17944, accessed June 22, 2023.

Nooksack Indian Tribe Natural Resources Department (NNR). 2015. South Fork Nooksack (Nuxw7íyem) Nesset Phase 1 Restoration. Salmon Recovery Funding Board Project #15-1283. Washington State Recreation and Conservation Office, Olympia, WA, available at https://srp.rco.wa.gov/project/360/29581, accessed Nov. 18, 2022.

Nooksack Indian Tribe Natural Resources Department (NNR). 2016. South Fork Nooksack (Nuxw7íyem) Nesset Phase 2 Restoration. Salmon Recovery Funding Board Project #16-2049. Washington State Recreation and Conservation Office, Olympia, WA, available at https://srp.rco.wa.gov/project/360/80475, accessed Nov. 18, 2022.

Pelto, M.S., Dryak, M., Pelto, J., Matthews, T., and L.B. Perry. 2022. Contribution of glacier runoff during heat waves in the Nooksack River basin USA. *Water* 14: 1145.

Poole, G.C., and C.H. Berman. 2001. An ecological perspective on in-stream temperature: natural heat dynamics and mechanisms of human-caused thermal degradation. *Environmental Management* 27: 787–802.

R Core Team. 2023. R: A language and environment for statistical computing. R Foundation for Statistical Computing, Vienna, Austria. Available: https://www.R-project.org/.

Richter, A., and S. A. Kolmes. 2005. Maximum temperature limits for Chinook, coho, and chum salmon, and steelhead trout in the Pacific Northwest. *Reviews in Fisheries Science* 13: 23-49.

Roni, P., K. Hanson, and T. Beechie. 2008. Global review of the physical and biological effectiveness of stream habitat rehabilitation techniques. *North American Journal of Fisheries Management* 28: 856-890.

Schoonmaker, P.K., T. Gresh, J. Lichatowich, and H.D. Radtke. 2003. Past and present Pacific salmon abundance: bioregional estimates for key life history stages. Pages 33-40 *in* J.G. Stockner (ed.), Nutrients in Salmonid Ecosystems: Sustaining Production and Biodiversity. American Fisheries Society, Bethesda, MD.

Soicher, A., T. Coe, and N. Currence. 2006. South Fork Nooksack River Acme-Confluence Reach Restoration Planning: Analysis of Existing Information and Preliminary Restoration Strategies. IAC #02-1500N Final Report. Nooksack Tribe Natural Resources Department. Deming, WA.

Tate, K.W., D.L. Lancaster, and D.F. Lile. 2007. Assessment of thermal stratification within stream pools as a mechanism to provide refugia for native trout in hot, arid rangelands. *Environmental Monitoring and Assessment* 124: 289–300.

Tonina, D., and J. M. Buffington. 2007. Hyporheic exchange in gravel bed rivers with pool-riffle morphology: Laboratory experiments and three-dimensional modeling. *Water Resources Research* 43: W01421. U.S. Environmental Protection Agency. (USEPA). 2016a. Final Project Report: EPA Region 10 Climate Change and TMDL Pilot—South Fork Nooksack

River, Washington. EPA/600/R-17/281. National Health and Environmental Effects Research Laboratory, Western Ecology Division, Corvallis, OR.

Torgersen, C.E., J.E. Ebersole, and D.M. Keenan. 2012. Primer for Identifying Cold-Water Refuges to Protect and Restore Thermal Diversity in Riverine Landscapes. EPA 910-C-12-001, U.S. Environmental Protection Agency Region 10, Seattle, WA.

U.S. Environmental Protection Agency (USEPA). 2016b. Qualitative Assessment: Evaluating the Impacts of Climate Change on Endangered Species Act Recovery Actions for the South Fork Nooksack River, WA. EPA/600/R-16/153. National Health and Environmental Effects Research Laboratory, Western Ecology Division, Corvallis, OR.

U.S. Environmental Protection Agency (USEPA). 2020. Impaired Waters and TMDLs in Region 10. https://www.epa.gov/tmdl/impaired-waters-and-tmdls-region-10, accessed March 11, 2021.

U.S. Geological Survey (USGS). 2022. SF Nooksack River at Saxon Bridge, WA – 12210000, August 6, 2022 - September 13, 2022. USGS: science for a changing world. https://waterdata.usgs.gov/monitoring-location/12210000/#parameterCode=00060&startDT=2022-08-06&endDT=2022-09-13.

van Vliet, M.T.H., F. Ludwig, J.J.G. Zwolsman, G.P. Weedon, and P. Kabat. 2011. Global river temperatures and sensitivity to atmospheric warming and changes in river flow. *Water Resources Research* 47: W02544.

Visual Crossing. 2022. Weather Data & API Global Forecast & History Data: Historical weather data for Acme, Washington. https://www.visualcrossing.com/weather-history/acme%20washington/metric/2022-08-06/2022-09-13.

von Biela, V. R., Bowen, L., McCormick, S. D., Carey, M. P., Donnelly, D. S., Waters, S., Regish, A. M., Laske, S. M., Brown, R. J., Larson, S., Zuray, S., & C. E. Zimmerman. 2020. Evidence of prevalent heat stress in Yukon River Chinook salmon. *Canadian Journal of Fisheries and Aquatic Sciences*, 77(12): 1878–1892.

Willson M.F., Gende S.M., and B.H. Marston. 1998. Fishes and the forest: expanding perspectives on fish-wildlife interactions. *BioScience* 48: 455–62.

Wondzell, S.M., J. LaNier, R. Haggerty, R.D. Woodsmith, and R.T. Edwards. 2009. Changes in hyporheic exchange flow following experimental wood removal in a small, low-gradient stream. *Water Resources Research* 45: W05406.

WRIA 1 Salmon Recovery Board (WRIA 1 SRB). 2005. Water Resources Inventory Area (WRIA) 1 Salmonid Recovery Plan. October 11, 2005. Bellingham, WA.

Yoder, J., and C. Raymond. 2022. Climate Change and Stream Flow: Barriers and Opportunities. Preliminary project report to the Washington State Department of Ecology. Water Resources Program, Washington State Department of Ecology, Olympia, Washington. June 2022, Publication 22-11-029.

Tables and Figures

Table 1: Locations and descriptions of study sites in Nesset's Reach, South Fork Nooksack River. Each site consists of a single engineered log jam (ELJ) and an associated ELJ-formed pool with a riffle immediately upstream. Piezometers and temperature loggers were installed at the riffle tail/pool head. Upwelling potential was assessed in terms of vertical hydraulic gradient (VHG), a unitless measure of the pressure differential between the hyporheic zone at the piezometer location and the overlying surface stream. Residual pool depth was calculated as the difference between the maximum water depth within the pool and the water depth at the pool tailout.

Site ID	Location (Latitude, Longitude)	Year ELJ built	Piezometer Installation depth (cm below streambed)	VHG	Residual pool depth (m)
1302	(48.689145 °N, -122.165981 °W)	2016	37.5	+1.0	1.34
1306	(48.689115 °N, -122.165132 °W)	2016	30.5	+1.0	1.89
1312	(48.691559 °N, -122.165912 °W)	2016	36.75	+2.5	0.76
1313	(48.692227 °N, -122.163613 °W)	2016	33.75	+1.5	>3.17
1316	(48.692887 °N, -122.163720 °W)	2016	33	+1.0	0.91
2124	(48.695461 °N, -122.166573 °W)	2018	32.75	+0.25	0.88

Table 2: Results of permutation tests comparing surface stream temperatures and underlying hyporheic temperatures at each hour of the day at each study site. Data presented are the mean surface – hyporheic difference in temperature (temp), where each temperature measurement represents the mean temperature for that hour, averaged over all days in the sample period. Significant differences ($p < 0.05$) are highlighted and marked with asterisks.

	Site 1302		**Site 1306**		**Site 1312**		**Site 1313**		**Site 1316**		**Site 2124**	
Time	**temp**	***p***	**temp**	***p***	**temp**	***p***	**temp**	***p***	**temp**	***p***	**temp**	***p***
12:00 AM	**.919**	**.019***	.226	.681	.143	.700	-.023	.942	**6.530**	**.001***	-.046	.903
1:00 AM	**.814**	**.031***	-.124	.804	.144	.722	-.032	.927	**6.296**	**.001***	-.052	.883
2:00 AM	.721	.075	-.448	.343	.127	.761	-.035	.928	**6.032**	**.001***	-.055	.875
3:00 AM	.629	.090	-.730	.139	.109	.775	-.036	.917	**5.770**	**.001***	-.059	.863
4:00 AM	.533	.165	-.980	.052	.085	.845	-.041	.923	**5.504**	**.001***	-.058	.879
5:00 AM	.438	.265	**-1.193**	**.021***	.049	.908	-.048	.880	**5.235**	**.001***	-.061	.873
6:00 AM	.348	.353	**-1.379**	**.011***	.012	.977	-.057	.877	**4.964**	**.001***	-.063	.855
7:00 AM	.298	.406	**-1.542**	**.012***	-.018	.958	-.055	.880	**4.719**	**.001***	-.060	.882
8:00 AM	.344	.286	**-1.632**	**.003***	-.034	.926	-.034	.938	**4.562**	**.001***	-.052	.886
9:00 AM	.584	.069	**-1.553**	**.004***	-.039	.894	.017	.960	**4.595**	**.001***	-.006	.992
10:00 AM	**.947**	**.001***	**-1.346**	**.012***	-.006	.983	.067	.843	**4.852**	**.001***	.033	.919
11:00 AM	**1.423**	**.001***	-.918	.072	-.012	.962	.101	.765	**5.376**	**.001***	.082	.799
12:00 PM	**1.947**	**.001***	-.367	.448	-.028	.920	.127	.712	**6.059**	**.001***	.105	.757
1:00 PM	**2.360**	**.001***	.386	.449	-.002	.996	.145	.688	**6.807**	**.001***	.129	.703
2:00 PM	**2.590**	**.001***	**1.198**	**.035***	-.034	.938	.131	.726	**7.557**	**.001***	.119	.711
3:00 PM	**2.604**	**.001***	**1.678**	**.003***	-.089	.826	.071	.874	**8.001**	**.001***	.076	.846
4:00 PM	**2.311**	**.001***	**1.948**	**.001***	-.246	.533	-.016	.975	**8.289**	**.001***	.007	.985
5:00 PM	**1.977**	**.001***	**1.869**	**.003***	-.143	.725	-.064	.900	**8.212**	**.001***	-.050	.924
6:00 PM	**1.614**	**.002***	**1.608**	**.006***	-.125	.757	-.104	.800	**7.920**	**.001***	-.085	.815
7:00 PM	**1.310**	**.005***	**1.332**	**.018***	-.080	.850	-.097	.818	**7.509**	**.001***	-.109	.770
8:00 PM	**1.170**	**.010***	**1.152**	**.042***	-.008	.986	-.052	.897	**7.208**	**.001***	-.092	.821
9:00 PM	**1.069**	**.012***	.985	.068	.051	.924	-.038	.918	**6.973**	**.001***	-.065	.878
10:00 PM	**.992**	**.010***	.761	.154	.112	.807	-.024	.959	**6.777**	**.001***	-.054	.896
11:00 PM	**.928**	**.021***	.503	.329	.137	.776	-.020	.965	**6.578**	**.001***	-.049	.883

Table 3: Results of paired t-tests comparing mean daily maximum temperature, averaged over all days in the sample period, between the surface stream and underlying hyporheic zone at each study site. Results presented include the test statistic (*t*), degrees of freedom (df), and p-value (*p*). Asterisks indicate statistically significant results ($p < 0.05$).

Site ID	Hyporheic temperature category	Sampling period	Mean hyporheic daily maximum (°C)	Mean surface stream daily maximum (°C)	Difference in means (°C)	*t*	df	*p*
1302	**COOL**	8/6/22 – 9/10/22	18.338	20.343	-2.00	-8.8	32	<<0.001*
1306	**COOL**	8/22/22 – 9/13/22	17.932	19.568	-1.64	-7.7	20	<<0.001*
1312	**WARM**	8/8/22 – 9/13/22	21.059	20.918	0.14	2.9	34	0.007*
1313	**WARM**	8/8/22 – 9/13/22	20.185	20.170	0.02	2.2	34	0.04*
1316	**COLD**	8/8/22 – 9/13/22	11.793	20.131	-8.34	-23.5	34	<<0.001*
2124	**WARM**	8/6/22 – 9/13/22	20.324	20.314	0.01	1.6	36	0.10

Table 4: Results of paired t-tests comparing mean seven-day average of the daily maximum temperature (7DADM), averaged over all days in the sample period, between the surface stream and underlying hyporheic zone at each study site. Results presented include the test statistic (*t*), degrees of freedom (df), and p-value (*p*). Asterisks indicate statistically significant results ($p < 0.05$).

Site ID	Hyporheic temperature category	Sampling period	Mean hyporheic 7DADM (°C)	Mean surface stream 7DADM (°C)	Difference in means (°C)	*t*	df	*p*
1302	**COOL**	8/6/22 – 9/10/22	18.520	20.545	-2.02	-10.2	26	<<0.001*
1306	**COOL**	8/22/22 – 9/13/22	18.089	19.698	-1.61	-22.5	14	<<0.001*
1312	**WARM**	8/8/22 – 9/13/22	21.315	21.223	0.09	3.4	28	0.002*
1313	**WARM**	8/8/22 – 9/13/22	20.475	20.461	0.013	3.4	28	0.002*
1316	**COLD**	8/8/22 – 9/13/22	11.795	20.426	-8.63	-27.9	28	<<0.001*
2124	**WARM**	8/6/22 – 9/13/22	20.549	20.541	0.008	2.6	30	0.01*

Table 5: Results of paired t-tests comparing mean daily temperature range, averaged over all days in the sample period, between the surface stream and underlying hyporheic zone at each study site. Results presented include the test statistic (*t*), degrees of freedom (df), and p-value (*p*). Asterisks indicate statistically significant results ($p < 0.05$).

Site ID	Hyporheic temperature category	Sampling period	Mean hyporheic daily range (°C)	Mean surface daily range (°C)	Difference in means (°C)	*t*	df	*p*
1302	**COOL**	8/6/22 – 9/10/22	2.612	4.129	-1.52	-10.3	32	<<0.001*
1306	**COOL**	8/22/22 – 9/13/22	0.869	3.772	-2.90	-12.7	20	<<0.001*
1312	**WARM**	8/8/22 – 9/13/22	4.596	4.477	0.12	2.6	34	0.01*
1313	**WARM**	8/8/22 – 9/13/22	3.849	3.852	-0.003	-0.4	34	0.80
1316	**COLD**	8/8/22 – 9/13/22	0.169	3.862	-3.69	-20.9	34	<<0.001*
2124	**WARM**	8/6/22 – 9/13/22	4.017	4.029	-0.012	-1.5	36	0.20

Table 6: Results of regression analyses assessing the effects of piezometer installation depth and vertical hydraulic gradient (VHG) on response variables. Response variables include the daily maximum temperature, the seven-day average of the daily maximum temperature (7DADM), and the daily temperature range. Results presented include the Adjusted R^2, F-statistic (F), degrees of freedom (df), and p-value (*p*).

Response Variable	Predictor Variable							
	Installation Depth				VHG			
	R^2	F	df	*p*	R^2	F	df	*p*
Daily Maximum	-0.152	0.340	1,4	0.591	-0.150	0.348	1,4	0.587
7DADM	-0.152	0.341	1,4	0.590	-0.149	0.353	1,4	0.584
Daily Range	0.062	1.329	1,4	0.313	-0.087	0.599	1,4	0.482

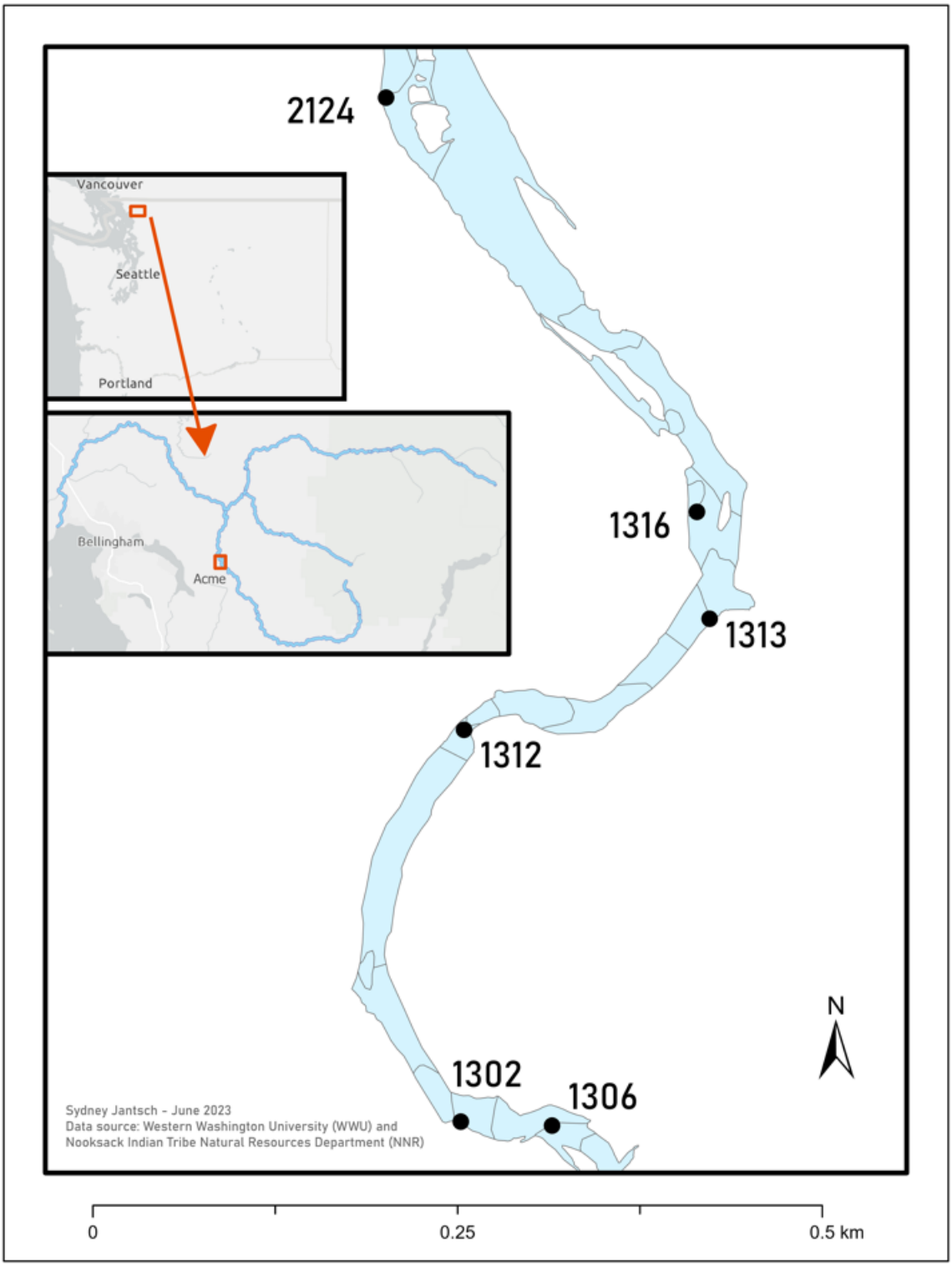

Figure 1. Study site locations in Nesset's Reach, South Fork Nooksack River. The top inset map depicts the location of the Nooksack River in Washington State. The lower inset map shows the full extent of the Nooksack River, with Nesset's Reach highlighted.

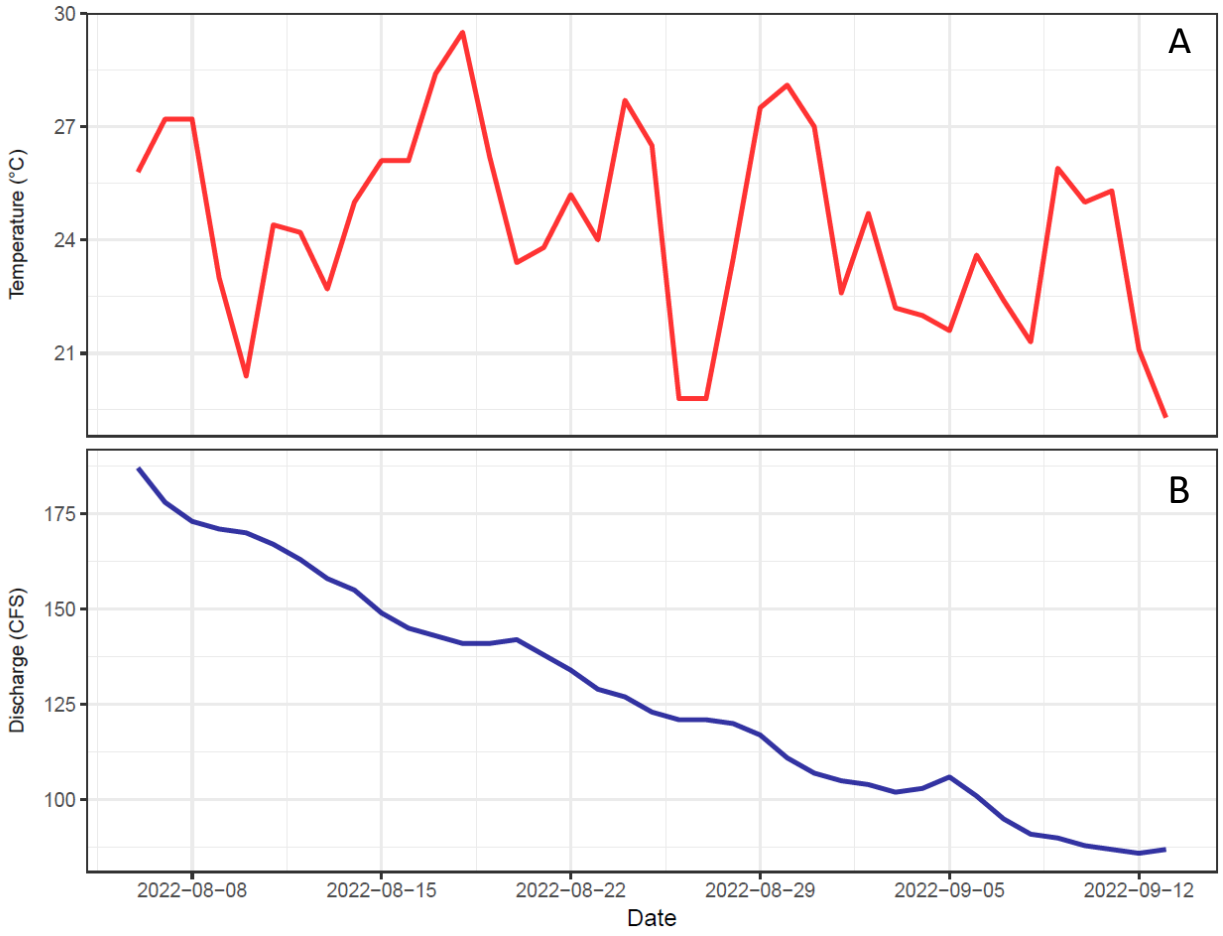

Figure 2. Maximum daily air temperature (A) and discharge (B) in the lower South Fork Nooksack River from August 6th to September 13th, 2022. Air temperatures were recorded in Acme, Washington (Visual Crossing 2022). Discharge was recorded at U.S. Geologic Service gauge 12210000 (SF Nooksack River at Saxon Bridge, WA), approximately 1.6 river km (1 river mile) upstream from Nesset's reach (USGS 2022).

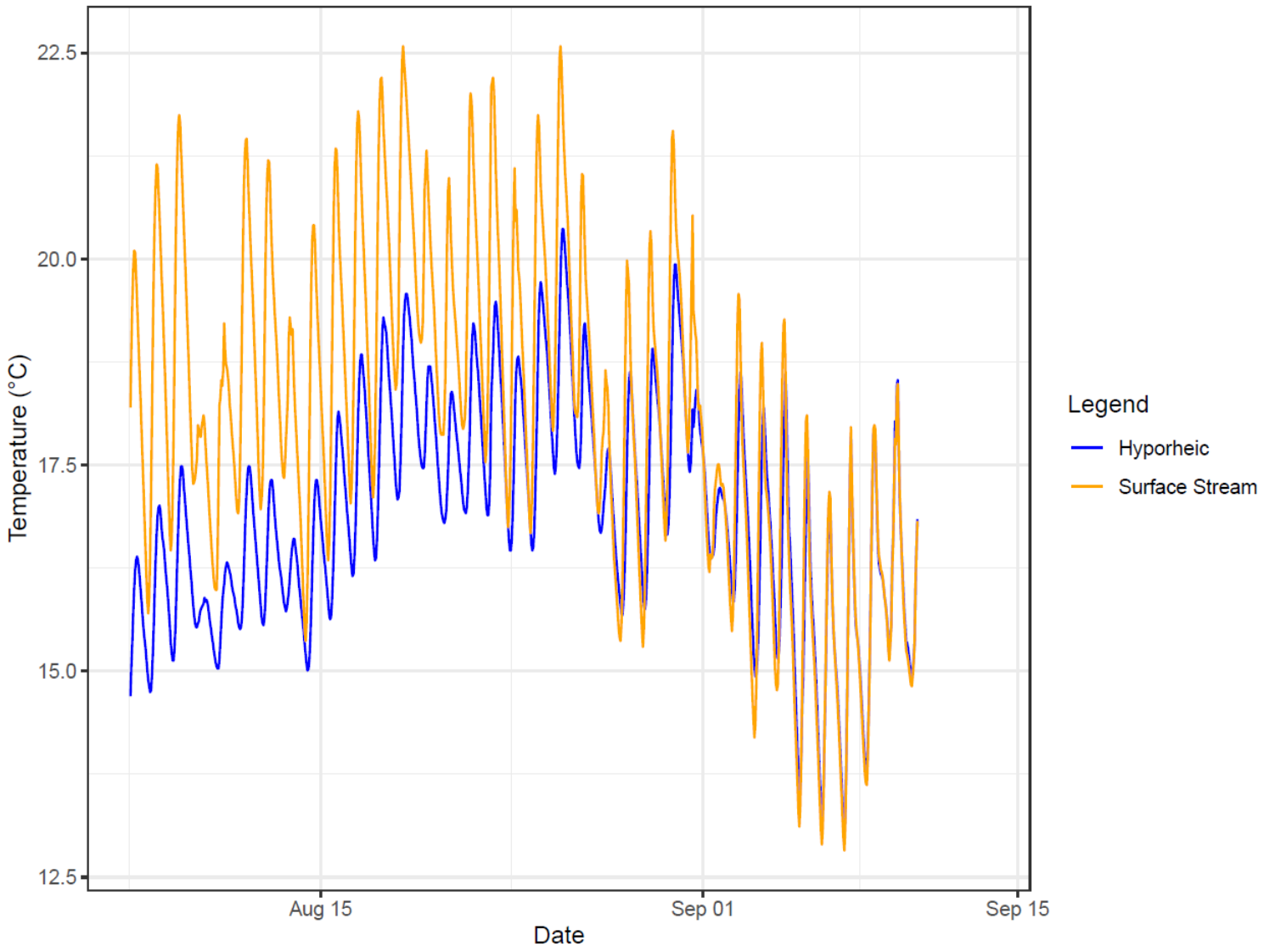

Figure 3. Hyporheic and surface stream temperatures at site 1302 in Nesset's Reach, South Fork Nooksack River, from August 6 to September 10, 2022.

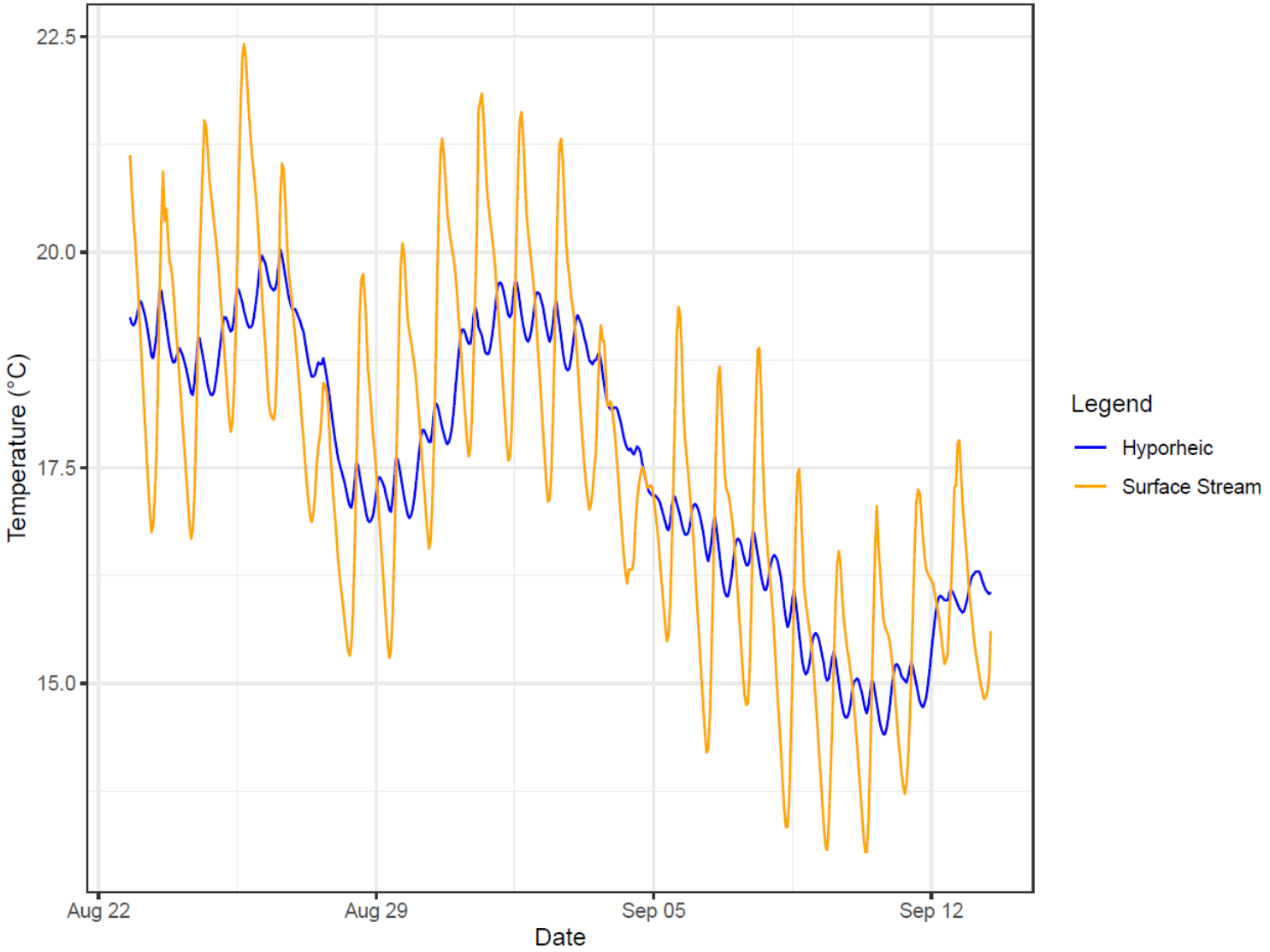

Figure 4. Hyporheic and surface stream temperatures at site 1306 in Nesset's Reach, South Fork Nooksack River, from August 22 to September 13, 2022.

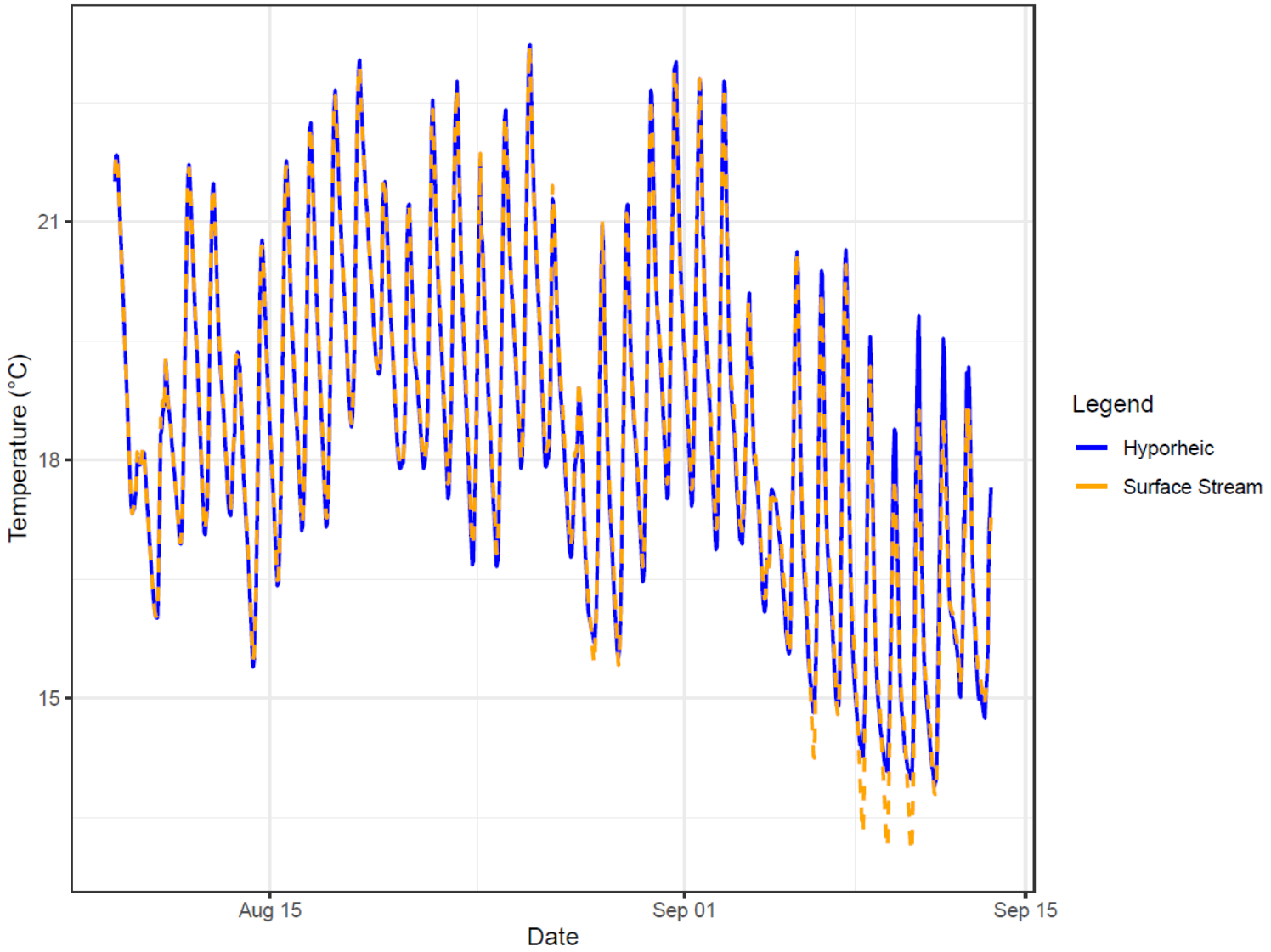

Figure 5. Hyporheic and surface stream temperatures at site 1312 in Nesset's Reach, South Fork Nooksack River, from August 8 to September 13, 2022.

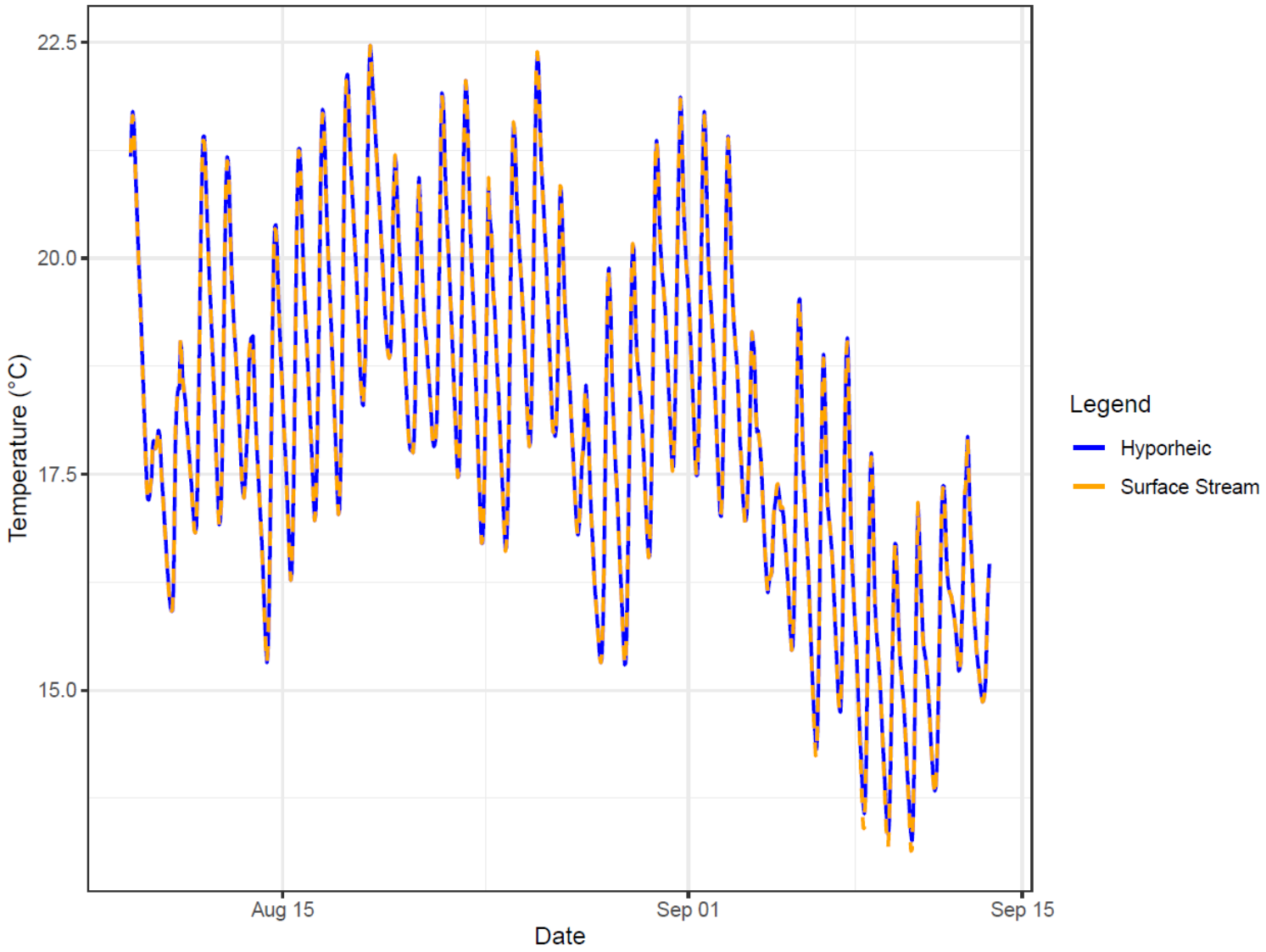

Figure 6. Hyporheic and surface stream temperatures at site 1313 in Nesset's Reach, South Fork Nooksack River, from August 8 to September 13, 2022.

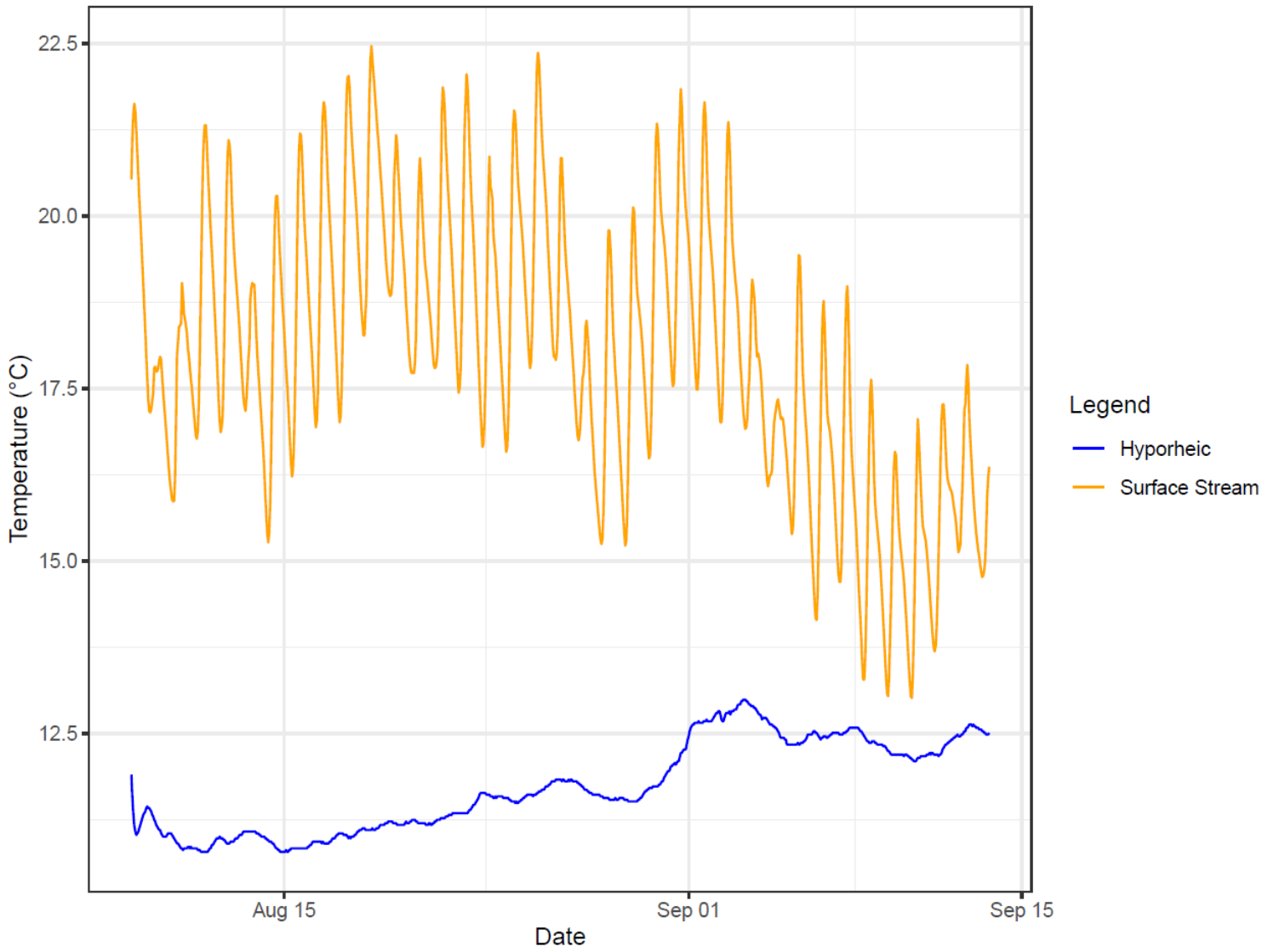

Figure 7. Hyporheic and surface stream temperatures at site 1316 in Nesset's Reach, South Fork Nooksack River, from August 8 to September 13, 2022.

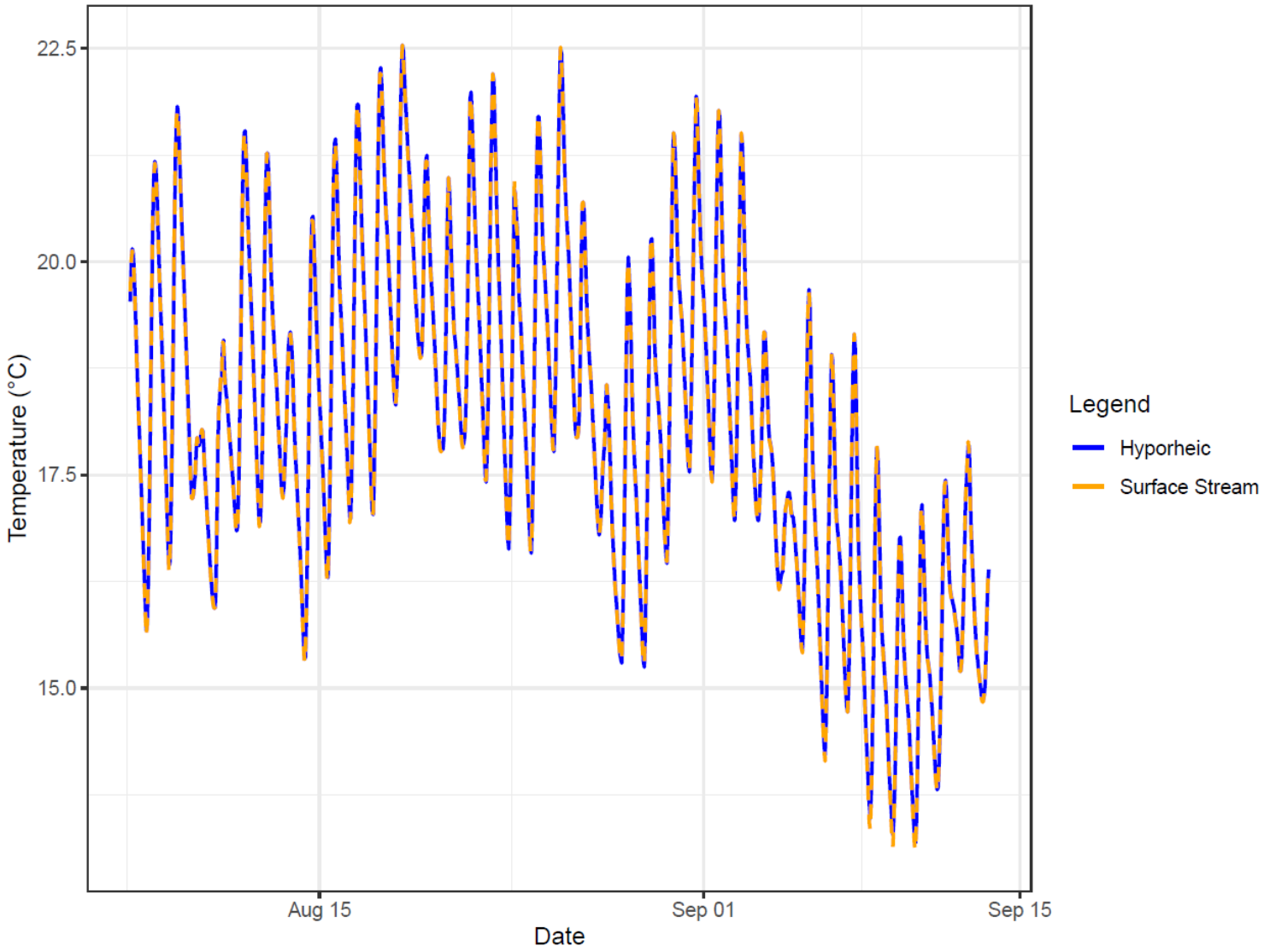

Figure 8. Hyporheic and surface stream temperatures at site 2124 in Nesset's Reach, South Fork Nooksack River, from August 6 to September 13, 2022.

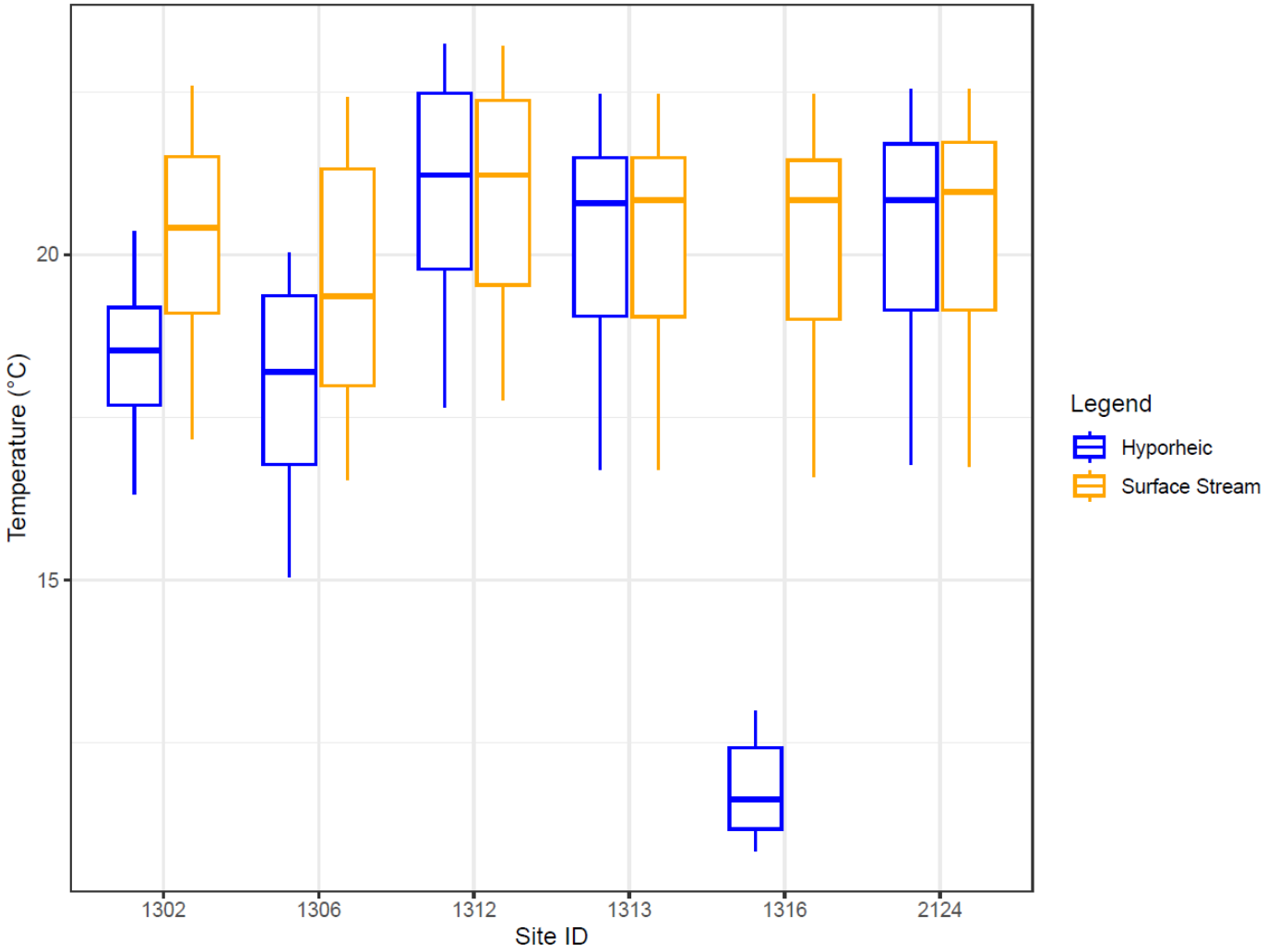

Figure 9. Boxplots of daily maximum hyporheic and surface stream temperatures at study sites in Nesset's Reach, South Fork Nooksack River, during the 2022 summer low-flow season (August 6 to September 13).

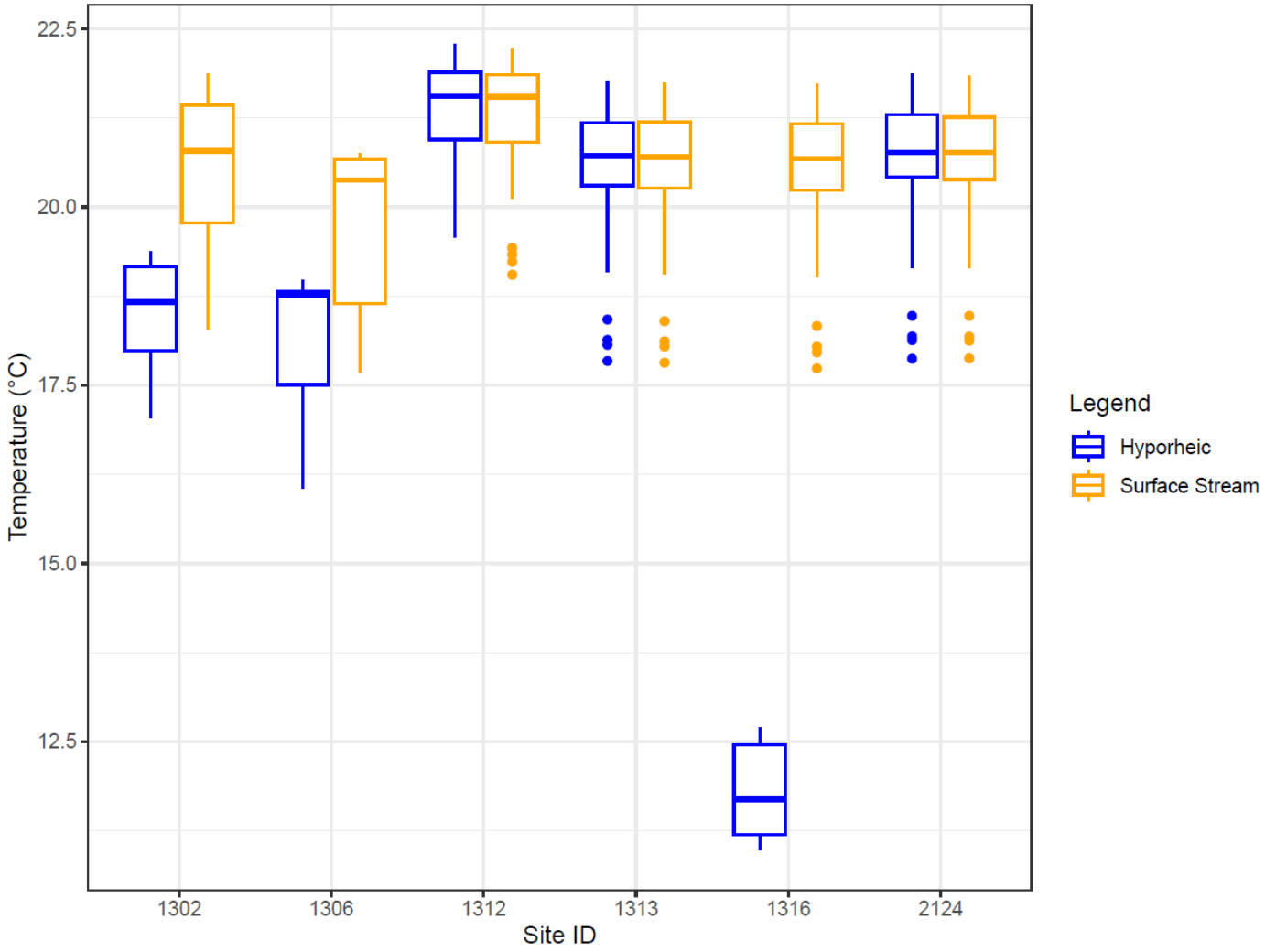

Figure 10. Boxplots of the seven-day average of the daily maximum (7DADM) hyporheic and surface stream temperatures at study sites in Nesset's Reach, South Fork Nooksack River, during the 2022 summer low-flow season (August 6 to September 13).

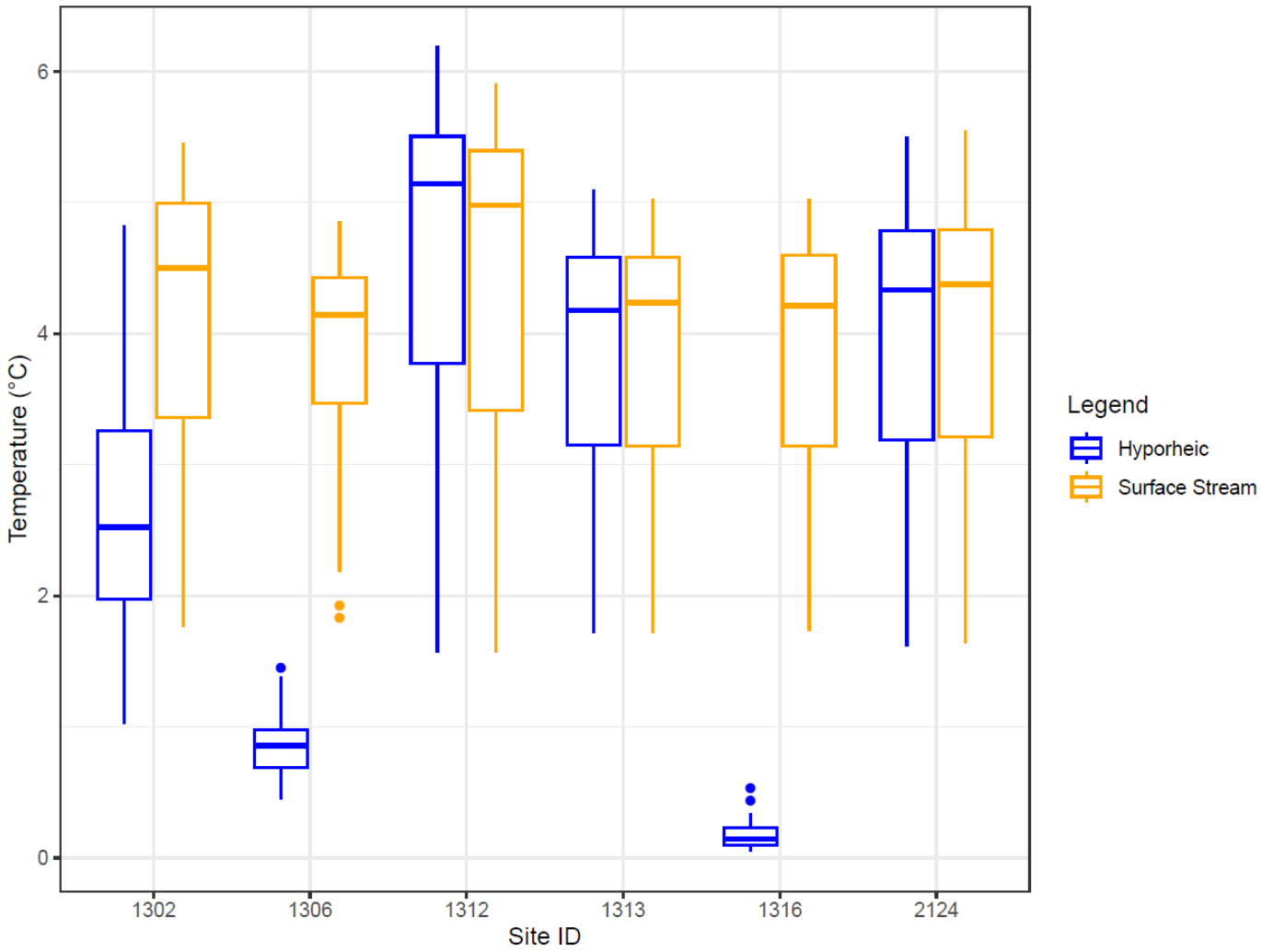

Figure 11. Boxplots of the daily range of hyporheic and surface stream temperatures at study sites in Nesset's Reach, South Fork Nooksack River, during the 2022 summer low-flow season (August 6 to September 13).

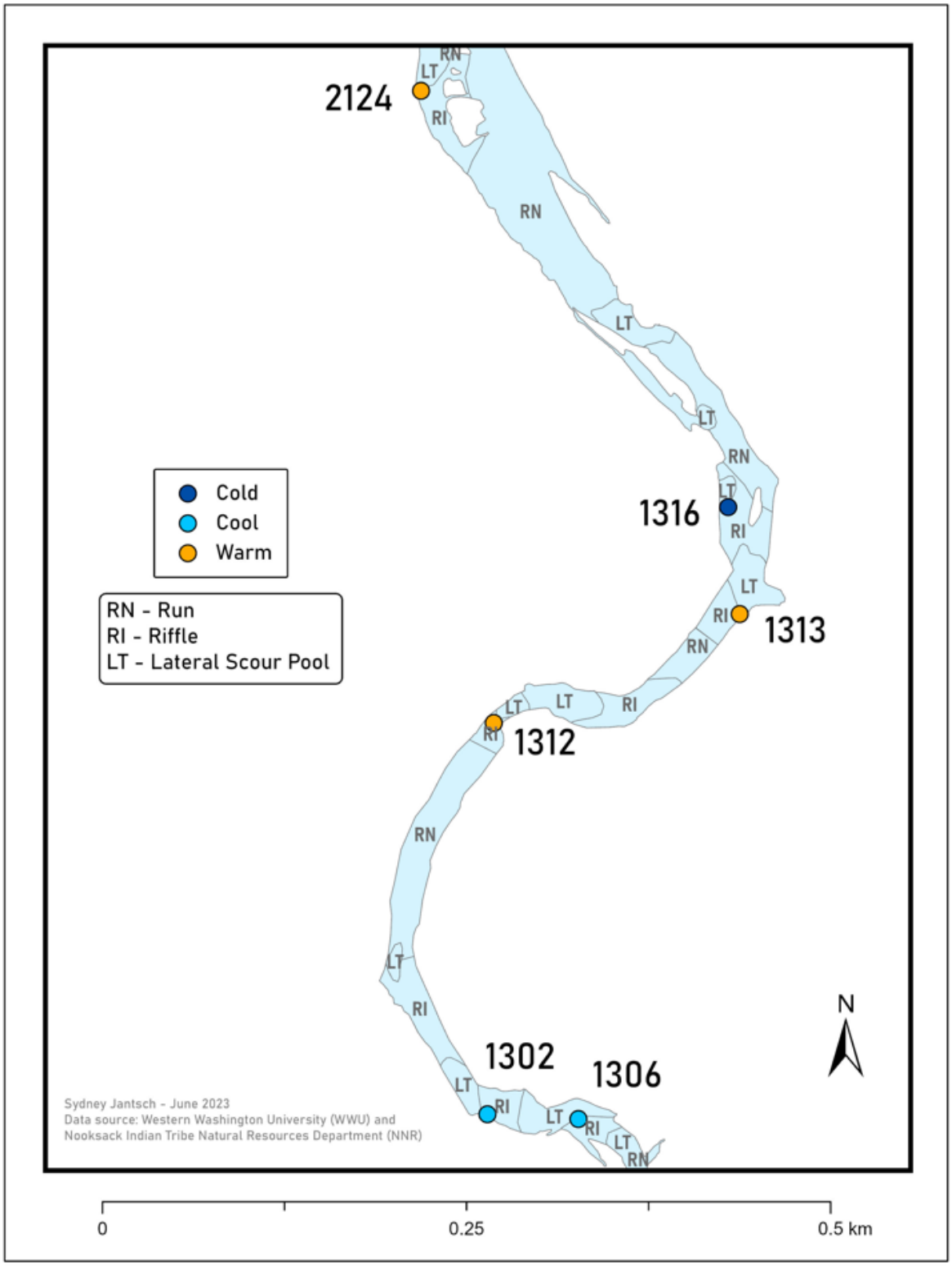

Figure 12. Study sites grouped by hyporheic temperature categories with surrounding channel geomorphic units in Nesset's Reach, South Fork Nooksack River.

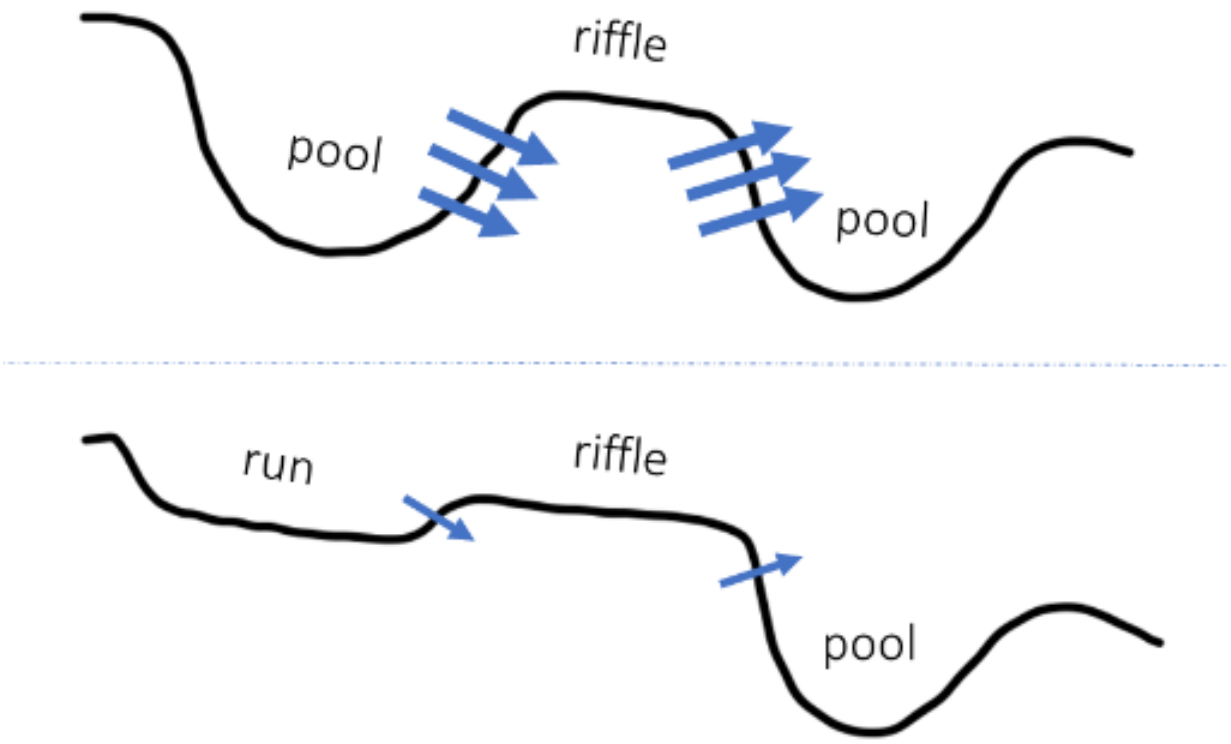

Figure 13. Profile diagram showing variations in channel morphology and hyporheic exchange. Blue arrows represent the direction of hyporheic exchange (i.e., upwelling vs. downwelling), with thicker arrows indicating greater flow rates.